Biophysical characterisation of LL-37-derived antimicrobial peptides

Ilišinović, Drago

Master's thesis / Diplomski rad

2016

Degree Grantor / Ustanova koja je dodijelila akademski / stručni stupanj: **University of Zagreb, Faculty of Pharmacy and Biochemistry / Sveučilište u Zagrebu, Farmaceutsko-biokemijski fakultet**

Permanent link / Trajna poveznica: https://urn.nsk.hr/urn:nbn:hr:163:963331

Rights / Prava: In copyright/Zaštićeno autorskim pravom.

Download date / Datum preuzimanja: **2024-07-12**

Repository / Repozitorij:

Repository of Faculty of Pharmacy and Biochemistry University of Zagreb

Drago Ilišinović

Biophysical characterisation of LL-37-derived antimicrobial peptides

DIPLOMA THESIS

Submitted to University of Zagreb Faculty of Pharmacy and Biochemistry

Zagreb, 2016.

CONTENTS

1. INTRODUCTION

In September 2016, world leaders have met at the United Nations (UN) to discuss the problem of antimicrobial resistance (AMR) (www.who.int). It was only the fourth time ever a health issue had been discussed at the UN General Assembly Combined with the fact that the World Health Organisation (WHO) has warned that "antimicrobial resistance threatens the very core of modern medicine and the sustainability of an effective, global public health response to the enduring threat from infectious diseases" (WHO, 2015), there are strong indications that antimicrobial resistance will be a major problem in future. Simultaneously, World Bank has reported that the worldwide increase of health system costs caused by AMR could cause similar effects on global economy to those of the 2008 financial crisis (World Bank, 2016).

Therefore, it is clear that measures need to be taken to rationalise the use of currently known antimicrobial drugs, as well as to develop new antimicrobials, in particular new antibiotics which could cure multiple drug resistant (MDR) bacterial infections. One class of chemical compounds that have antibiotic properties are antimicrobial peptides (AMPs), which are naturally occurring defence mechanisms against pathogens of most living organisms. These peptides act against a wide range of microorganisms, including Gram-positive and Gram-negative bacteria, mostly by disrupting the plasma membrane, which leads to cell lysis (Reddy et al., 2004). These peptides can then be used as models for synthesis of new peptides with different, new or enhanced properties.

1.1. ABOUT AMPs IN GENERAL AND THEIR APPLICATION AS THERAPEUTIC AGENTS IN TREATMENT OF BIOFILM ASSOCIATED INFECTIONS

Antimicrobial peptides offer protection to various organisms against pathogens such as viruses, bacteria and fungi. Considering their antibacterial activity, the majority of peptides do not target a single target as conventional antibiotics, but instead act directly on the cytoplasmic membrane. Therefore, their activity is independent of bacterial metabolic activity. They act as microbicides within minutes of contact and, since they have no specific target on which they act, bacterial resistance is less likely to be developed (Zasloff, 2002). They are also biodegradable.

In addition to having antimicrobial properties, some of these peptides also possess other properties, such as immunomodulatory and anti-inflammatory action, bacterial cell components–neutralising activity and biofilm–eradicating properties (Hancock and Sahl, 2006). Considering their structure, they are usually short (up to 40 amino acid residues), cationic, amphipathic and often helical. (www.bali-consortium.eu)

It has been found that certain AMPs have anti-biofilm properties (Batoni et al., 2016). Biofilms are aggregates of microorganisms in which cells are embedded within a self-produced matrix of extracellular polymers and in which they adhere to each other and/or the surface (Vert et al., 2012). Infections involving biofilms are very hard to eradicate as the biofilm offers protection against both the host's immune system and conventionally applied antibiotics. Biofilms can form on prosthetic medical devices that are surgically implanted into a patient's body, such as artificial heart valves, artificial hips, joints etc. It can be especially dangerous if an infection occurs with a resistant or multiple-resistant bacterial strain, such as methicillin-resistant *Staphylococcus aureus* (MRSA). This can cause chronic, severe infections.

An international consortium called Biofilm Alliance (BALI) has been established with the goal of developing antimicrobial peptides that would be coated on prosthetic implants with controlled release in hope of preventing biofilm-associated infections and improving patients' quality of life (www.bali-consortium.eu). Biofilm Alliance (BALI) project uses OP-145 as a model for the development of novel AMPs with better properties to fight against biofilm-associated infections (www.bali-consortium.eu). OP-145 (previously known as P60.4Ac) is

an antimicrobial peptide that was developed from LL-37 (Nell et al., 2006). LL-37 belongs to a family of the naturally occurring peptides called cathelicidins (Zanetti et al., 1995). It is a 37-residue product of proteolytic degradation of the human cathelicidin hCAP-18 (Sørensen et al., 1997). LL-37 is an amphipathic, α-helical peptide found throughout the body with antibacterial, immunomodulatory and lipopolysaccharide (LPS)-neutralising activity (Bucki et al., 2008; Dürr et al., 2006).

1.2. MEMBRANE COMPOSITION AS A KEY FACTOR OF PEPTIDE SPECIFICITY: MODEL MEMBRANES

As mentioned before, most antimicrobial peptides manifest their effect by acting upon the cell membrane Therefore, membranes and their composition are of special interest when discussing AMPs.

Prokaryotic and eukaryotic membranes have different lipid composition. Indeed, even different bacterial species may differ in lipids present in their membranes. It is this composition that is crucial to AMPs activity, in addition to the nature of the peptide, as they may be more selective towards certain kinds of lipids because of their charge or hydropathicity (Koller and Lohner, 2014; Lohner, 2009).

Gram-negative cell envelope consists of two lipid bilayers, the outer membrane and the inner membrane. The outer membrane is highly asymmetrical, with lipopolysaccharides located exclusively on the outer side, and phospholipids, most of which phosphatidylethanolamine (PE), on the inner side. On the other hand, the inner membrane is composed mostly of PE and, to a lesser extent, negatively charged lipids such as phosphatidylglycerol (PG). In between them lies a layer of peptidoglycan (PGN). Gram-positive bacteria have only the inner membrane of similar composition, but with more PG than PE and with a thick layer of PGN and lipoteichoic acid (LTA) on the outside (Lohner et al., 2008).

Eukaryotic cell membranes show high asymmetry, with amino phospholipids such as PE and phosphatidylserine (PS) occupying almost exclusively the inner side, while the outer side is rich in choline phospholipids, mostly zwitterionic phosphatidylcholine (PC) and sphingomyelin (SM). This asymmetry is maintained by an ATP-dependent translocase. In

physiological conditions, PS presence on the surface of a cell membrane is an apoptotic signal for the immune system to get rid of the cell. However, PS is present on cell surface also in certain pathological conditions, primarily in cancerous cells. Therefore, it has been investigated as a target for anticancer therapy (Riedl et al., 2015). A high content of cholesterol of around 25% is also characteristic for animal membranes (Lohner et al., 2008).

It is also worthy to note that bacterial and mammalian membranes alike are a complex mixture not just of various lipids, but of different peptides and polysaccharides also. While lipid composition is the main factor, other membrane components may add or subtract to AMP's activity. Membrane domains are also something worth describing. An AMP may prefer to interact with one lipid species over the other. Therefore, in a membrane composed of various lipids, it may happen that a membrane domain composed only of one lipid species is formed beneath the peptide, such as in a carpet model. Such lipid segregation may lead to membrane destabilisation and consequently disruption because of, for example, changed surroundings of membrane proteins or different curvature of the membrane (Lohner et al., 2008).

Bacterial cell envelope also needs to be taken into consideration. It has recently been discussed that the PGN layer of Gram-positive bacterial cells does not have an influence on antimicrobial activity, whereas interaction with LTA diminishes the concentration of peptide on the membrane itself, possibly by the mostly positive AMPs binding to the negatively charged LTA (Malanovic and Lohner, 2016).

Given the complexity of biological membranes, there is a need for their simplification in biophysical research. In this thesis, the membrane activity of peptides was studied on prokaryotic and eukaryotic model membranes. PG liposomes were used to mimic Gram-positive bacterial cell membranes, and PC liposomes to mimic mammalian cell membranes. These lipids were prepared in such a way that they formed liposomes. Liposomes can come in the form of multilamellar vesicles (MV), oligolamellar vesicles (OV) and unilamellar vesicles (UV), depending on the number of lipid bilayers inside one vesicle. For certain experiments it is vital that the liposomes are unilamellar, so they need to be extruded through membrane filters (Zweytick et al., 2011). SDS and DPC micelles, which are good approximations of bacterial and mammalian model membranes, respectively, were used too (Manzo et al., 2013). However, care needs to be taken when results taken from research on model systems are

compared to the activity on real cells as the role of individual lipid species and the affinity with which AMPs bind to them is not yet fully understood (Lohner et al., 2008).

1.3. MECHANISM OF ACTION OF AMPs: THE CASE OF OP-145 – MEMBRANE INTERACTION

It has been shown that AMPs exert their action mostly by acting upon bacterial cytoplasmic membrane, causing it to destabilise and disrupt (Lohner, 2009; Reddy et al., 2004). Two major models are discussed in literature: the carpet mechanism and transmembrane pore-forming mechanism (Lohner et al., 2008). In the carpet mechanism, peptides gather on the membrane surface because of electrostatic interactions and, upon reaching a critical concentration, exert their action by either a detergent-like effect or some other destabilising mechanism. In the other model, peptides arrange themselves through the membrane in a way a pore is formed which causes cell content leakage, whereas the membrane itself might stay intact, although membrane thinning through mechanisms such as interdigitation or *trans-gauche* isomerisation might precede pore formation (Koller and Lohner, 2014; Lohner et al., 2008). An overview of these modes of action is given on Figure 1. It is the phenomenon of interdigitation that is of special interest as it has been shown that OP-145 interacts with model membranes in such a way. In essence, in a lipid bilayer, lipids are oriented with their hydrocarbon chains towards one another to form a hydrophobic core. When interdigitation occurs, lipids are pushed towards each other vertically so that long hydrocarbon chains of lipids from opposite sides are intertwined, either partially or completely. This causes membrane thinning and destabilisation (Smith and Dea, 2013). A graphical representation of this process is provided on Figure 2. Other mechanisms may be involved, too, and it is suggested that these different mechanisms are gradual steps in the process of membrane destabilisation (Lohner and Prenner, 1999).
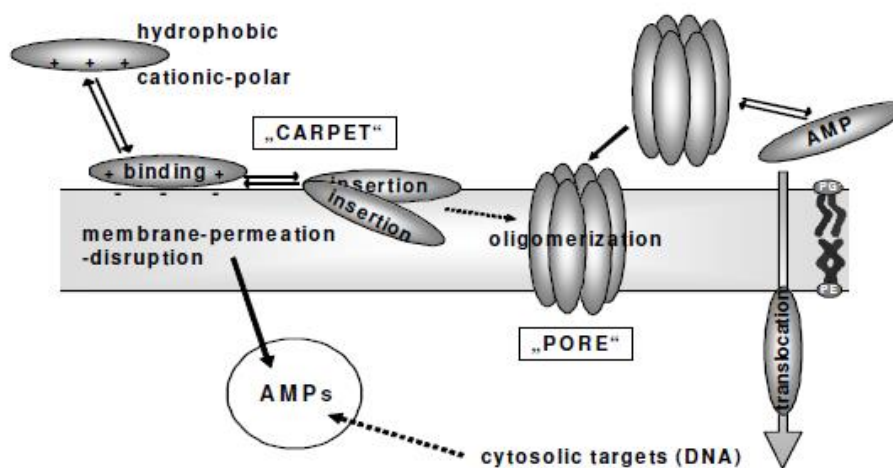
Figure 1. An overview of AMPs modes of action (retrieved from www.bali-consortium.eu).
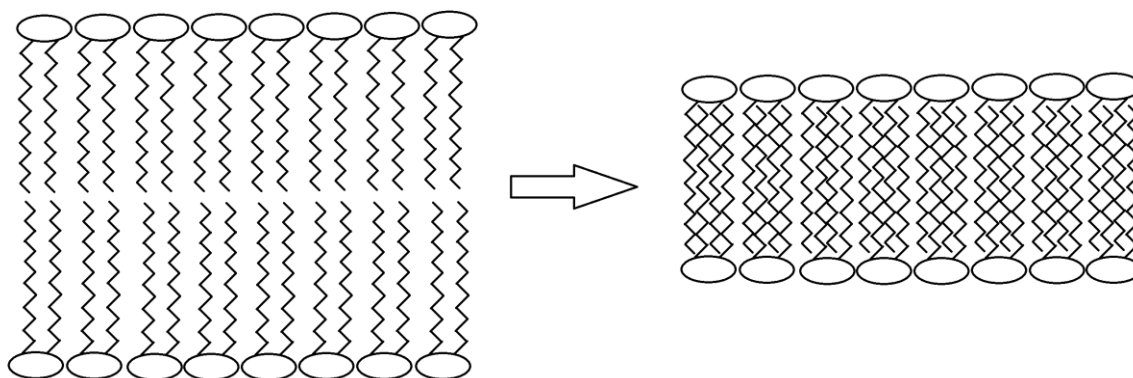
Figure 2. A simplified scheme of interdigitation process.

1.4. RATIONALE BEHIND DESIGN OF AMPs BASED ON OP-145

OP-145 is a 24-residue peptide developed at the Leiden University Medical Center (LUMC), Leiden, The Netherlands (Nell et al., 2006) with the sequence acyl-LKRVWKRVFKLLKRYWRQLKKPVR-amide. It has been shown that OP-145 possesses activity against Gram-positive bacteria such as methicillin-resistant *S. aureus* (MRSA) (Haisma et al., 2014) and that it has low toxicity towards mammalian cells (Malanovic et al., 2015). Moreover, it has anti-inflammatory and biofilm-eradicating properties (Nell et al., 2006) and has been shown to be safe and efficient in the treatment of chronic otitis media in clinical Phase I and II trials (Peek et al., 2009). It has been suggested for use in prosthetic implants as a coating which would protect both against infection and biofilm formation (de Breij et al., 2016). However, it also has certain disadvantages, such as propensity towards bacterial enzymatic degradation and, especially, considerably low level of activity in presence

of blood plasma. LC$_{99.9}$ (the lowest concentration that kills 99.9% of bacteria) of OP-145 in phosphate-buffered saline (PBS) was determined to be 1.6 µM, whereas in 50% plasma in PBS it was about 204.8 µM (Nibbering, 2015).

As mentioned earlier, BALI project aims to develop new, improved AMPs based on OP-145 with better properties: greater specificity for prokaryotic membranes, resistance to degradation, improved antimicrobial, antibiofilm and immunoorchestrating activities, lower cytotoxicity, resistance to proteolysis by bacterial enzymes, larger level of activity in presence of blood plasma and improved safety and efficacy. Among the peptides developed by this consortium are P148 and P276, whose characterisation is the main subject of this thesis.

1.5. P148 AND P276: NOVEL PEPTIDES WITH IMPROVED PROPERTIES

P148 and P276 are peptides derived from OP-145 with following sequences:

P148: acyl-LKRVWKRVFKLLKRYWRQLKKPVR-amide and
P276: acyl-LKRVWKAVFKLLKRYWRQLKKPVR-amide.

They differ mutually only in the 7th amino acid residue (alanine in P276 instead of arginine found in P148), as P276 was developed from P148 via alanine scanning (Nibbering, 2015). P148 and P276 were designed to fold into an alpha helix with all the hydrophobic residues on one side of the helix and the cationic ones on the other – an amphipathic helix (Nibbering, 2015). In comparison to OP-145, both novel peptides are characterized by higher net positive charge and higher total hydrophobicity, which is considered to be important for initial binding to anionic membrane phospholipids and higher partitioning into membrane. This certainly would lead to stronger membrane disruption.

Both novel peptides, P148 and P276, exhibit similar antimicrobial activity in PBS as tested in comparison to OP-145 (Nibbering, 2015). Interestingly, they show significant increase in killing of both Gram-positive and Gram-negative bacteria in the presence of 50% plasma. This is an advantage of the novel peptides compared to OP-145 which loses its activity in presence of blood plasma. Their haemolytic activity on human erythrocytes (experiments were performed in a cooperating laboratory: Anna de Breij, Leiden University Medical

Centre, Leiden, The Netherlands) is higher than for OP-145, but they are not haemolytic at the concentration where they exert antimicrobial activity. In conclusion, this observation suggests the novel peptides as better candidates for applications in humans.

Table 1. OP-145, P148 and P276 activity against *Staphylococcus aureus* and *Pseudomonas aeruginosa.* The results are expressed as a lethal concentration ($LC_{99.9}$) that kills 99.9% bacterial cells within 2 h.

| | LC99.9 (µM) | | | | | |
| | PBS | | | 50% plasma | | |
	OP-145	P148	P276	OP-145	P148	P276
S. aureus JAR060131 (G+)	1.60	1.60	0.80	204.8	12.8	6.4
P. aeruginosa PAO1 (G-)	3.2	1.6	0.8	>204.8	12.8	51.2

Table 2. OP-145, P148 and P276 haemolytic activity. Results are presented as median maximal non-haemolytic concentration (MMNHC).

| | Median maximal non-haemolytic concentration (µM) | |
	PBS	50% plasma
OP-145	1.6 (0.8-3.2)	51.2
P148	0.3 (0.2-0.8)	12.8 (6.4-25.6)
P276	0.2	12.8

2. RESEARCH OBJECTIVES

Resistance to antimicrobial drugs is an ever-growing problem in modern healthcare. Since the introduction of penicillin in 1943, nearly every antibiotic has seen at least one bacterial strain develop a resistance (http://www.cdc.gov). Therefore, there is a need for research of new antibiotics. One approach in this area is researching novel antimicrobial peptides (AMPs) (Lohner, 2009). These peptides are often derivatives of naturally occurring peptides, which exhibit action against microorganisms. One such peptide is a human cathelicidin LL-37 derivative, OP-145 (Malanovic et al., 2015; Nell et al., 2006), whose derivatives P148 and P276 were studied in this thesis.

The goal of this thesis was to study the biophysical properties of P148 and P276 and the way they interact with bacterial and mammalian model membranes, simulating their action on prokaryotic and eukaryotic cell membranes. These properties were then compared with those of OP-145. In addition, the purpose was to deepen the knowledge of antimicrobial peptides and to contribute to the global fight against microbial antibiotic resistance.

3. MATERIALS AND METHODS

3.1. MATERIALS AND INSTRUMENTS

The experiments that laid foundation for this thesis were performed using the following equipment:

- Heidolph MR 3001 K magnetic stirring hotplate, Heidolph Instruments GmbH & Co. KG, Germany
- Heidolph Reax top shaker/vortex, Heidolph Instruments GmbH & Co. KG, Germany
- Heraeus VTR5022 vacuum oven, Heraeus Holding GmbH, Germany
- Binder ED-53 and Binder FD-53 drying ovens, Binder GmbH, Germany
- Techne Dri-Block® DB200/3 sample concentrator, Bibby Scientific Ltd, UK
- Malvern Zetasizer Nano ZEN5600, Malvern Instruments Ltd, UK
- VP-DSC microcalorimeter, Microcal Inc., USA
- NanoDrop® spectrophotometer ND-1000, NanoDrop Technologies Inc., USA
- J-715-150S spectropolarimeter, JASCO Corp., Japan
- Cary Eclipse fluorescence spectrophotometer, Varian Australia Pty Ltd, Australia
- Electronic balance ABJ 220-4M, KERN & Sohn GmbH, Germany
- FiveEasy™ FE20 pH meter, Mettler-Toledo AG, Switzerland
- Avanti Mini Extruder with 0.1 μm polycarbonate membrane filters, Avanti Polar Lipids, Inc., USA
- Whatman™ 0.1 μm pore size nylon syringe filter, GE Healthcare Life Sciences, UK
- PIPETMAN® pipettes, Gilson S.A.S., France
- Elga LabWater PURELAB UHQ water purification system, Veolia Water, France.

Data was processed using the following software:

- Origin®, versions 7E and 9.3, OriginLab™, Microcal Inc., USA
- Zetasizer Software 7.02, Malvern Instruments Ltd, UK
- NanoDrop® ND-1000 v3.5.2, Coleman Technologies, Inc. for NanoDrop Technologies, Inc., USA
- Spectra Manager for Windows 95/NT, JASCO Corp., Japan

- Cary Eclipse Kinetics Applicaton v1.1 (133), Varian Australia Pty Ltd, Australia
- WebLab ViewerPro 4.0, Molecular Simulations Inc., USA
- DichroWeb, Institute of Structural and Molecular Biology, Birkbeck College, University of London, UK.

Following chemicals were used in the experiments:

- OP-145, P148 and P276, peptides (Nell, et al., 2006; Nibbering, et al., 2015)
- Sodium dihydrogen phosphate monohydrate p.a., Merck KGaA, Germany
- Disodium hydrogen phosphate ≥99% p.a., Carl Roth GmbH & Co. KG, Germany
- 4-(2-Hydroxyethyl)piperazine-1-ethanesulfonic acid (HEPES) min. 99.5%, Sigma-Aldrich Co., USA
- 1,2-dipalmitoyl-*sn*-glycero-3-phosphocholine (DPPC), Avanti Polar Lipids, Inc., USA
- 1,2-dipalmitoyl-*sn*-glycero-3-phospho-*rac*-(1-glycerol) sodium salt (DPPG), Sigma-Aldrich Co., USA
- 1-palmitoyl-2-oleoyl-*sn*-glycero-3-phosphocholine (POPC), Avanti Polar Lipids, Inc., USA
- 1-palmitoyl-2-oleoyl-*sn*-glycero-3-phospho-*rac*-(1-glycerol) sodium salt (POPG), Sigma-Aldrich Chemie GmbH, Germany
- 8-aminonaphthalene-1,3,6-trisulfonic acid, disodium salt (ANTS) and p-xylene-bis-pyridinium bromide (DPX), Molecular Probes™, Thermo Fisher Scientific, USA
- Sephadex™ G-75, GE Healthcare Life Sciences, UK
- Cholesterol, Sigma Grade, ≥99%, Sigma-Aldrich Co., USA
- Peptidoglycan (PGN) from *Bacillus subtilis*, Sigma-Aldrich Co., USA
- Triton™ X-100, laboratory grade, Sigma-Aldrich Co., USA
- Dodecylphosphocholine (DPC), Avanti Polar Lipids, Inc., USA
- Sodium lauryl sulfate (SDS) ≥99%, for biochemistry, Carl Roth GmbH & Co. KG, Germany
- Sodium lauryl sulfate ≥98.5%, BioReagent, suitable for electrophoresis, for molecular biology, Sigma-Aldrich Chemie GmbH, Germany
- 2-propanol ROTIPURAN® ≥99.8% p.a., ACS, ISO, Carl Roth GmbH & Co. KG, Germany
- Ethanol absolute p.a., AustrAlco Österreich Alkoholhandels GmbH, Austria

- Chloroform HPLC grade, J.T. Baker®, Mallinckrodt Baker B.V., Holland
- Bovine serum, Sigma-Aldrich Handels GmbH, Austria
- Bovine serum albumin (BSA) standard, Thermo Scientific, USA.

3.2. METHODS: PRINCIPLES OF TECHNIQUES USED IN EXPERIMENTS

In biophysical research of peptides and their interactions with model membranes a number of techniques are used. These include, but are not limited to, differential scanning calorimetry (DSC) (Smith and Dea, 2013), dynamic light scattering (DLS) (Stano et al., 2005), circular dichroism (CD) (Malanovic and Lohner, 2016) and fluorescent spectroscopy (Zweytick et al., 2011). These techniques were used to conduct experiments for this thesis and an overview of principles of their action is given below.

3.2.1. DIFFERENTIAL SCANNING CALORIMETRY (DSC)

DSC is a versatile thermoanalytical technique that can be used to analyse both solid and liquid samples in order to detect phase transitions. In analyses of liposomes, it can easily detect phase transitions and thermodynamic behaviour of pure lipids and lipid mixtures, including lipids organised into liposomes (Smith and Dea, 2013). DSC measures the difference in the amount of heat required to maintain both the sample and the reference at the same temperature. As phase transitions are either endothermic or exothermic processes, they require additional or reduced energy to keep the sample at the same temperature as the reference, and this difference is recorded in the thermogram. Both transition temperature and heat capacity can be determined this way (Atkins and de Paula, 2006).

Disaturated lipids organised in bilayers exhibit two different transitions: the so-called pre-transition in which they pass from the planar gel phase into the rippled gel phase and the main transition, when lipids pass from the gel phase into the fluid phase. The temperature range of the pre-transition is quite broad and is characterized by a lower enthalpy change than the main transition, which occurs at a higher temperature, is much sharper and more prominent on the thermogram and has higher enthalpy. Both pre-transition and main transition are affected

when lipids, i.e. liposomes interact with peptides: there can be a shift in temperature, an increase or a decrease in enthalpy and/or peak splitting, the last change indicating that different lipid domains have formed (Lohner and Prenner, 1999).

3.2.2. CIRCULAR DICHROISM (CD)

CD is the difference in the absorption of left- and right-hand polarised light. The difference is due to the properties of optically active molecules and to the three-dimensional structure of the polymer, if it is a polymer's such as a peptide's CD spectrum that is measured. Most notable use of this technique is the determination of secondary structure of peptides. Different secondary structures give different spectra in the UV region; therefore, from the relevant spectra of protein or peptide samples, their secondary structure can be determined (Atkins and de Paula, 2006). The results are usually expressed as mean residue molar ellipticity, $[\theta]_{MR}$, which is defined as ellipticity of the resultant polarised light vector per concentration of sample, cell pathlength and number of peptide bonds in the molecule (www.photophysics.com). Since it has been shown that the secondary structure of peptides influences the way peptides interact with membranes, it is often useful to determine secondary structure of AMPs in the presence and absence of lipid membranes in order to assess their activity (Arouri et al., 2013).

3.2.3. DYNAMIC LIGHT SCATTERING (DLS)

DLS, also known as quasi-elastic light scattering (QELS), is a technique used for measuring the size and size distribution of particles in the submicron range. It measures the hydrodynamic (Stokes) diameter of a given particle, meaning the diameter of a perfect sphere that diffuses in the same manner as the particle being measured. It takes into account solvatisation of the particle. DLS measuring results are expressed as Z-Average size, which is defined as the "harmonic intensity averaged particle diameter" (www.malvern.com) and given by default as intensity distribution. Polydispersity index (PDI) is a number between 0 and 1 and defines the measure of size distribution width, with lower values indicating a more uniform particle size distribution (www.malvern.com).

3.2.4. FLUORESCENCE SPECTROPHOTOMETRY (FLUOROMETRY)

This assay is based upon the principle of measurement of fluorescence from a fluorescent molecule (a fluorophore) when excited by exterior electromagnetic radiation. The exciting photons are generally from the UV range, while emission typically occurs in the visible part of spectrum (Watson, 1999).

One well-established assay uses 8-aminonaphthalene-1,3,6-trisulfonic acid (ANTS) as a fluorophore and p-xylene-bis-pyridinium bromide (DPX) as a quencher. A quencher is a molecule that shortens the lifetime of the excited state of a fluorophore, that is, quenches fluorescence (Atkins and de Paula, 2006). ANTS and DPX are present together in a liposome that is to be analysed; therefore, the fluorescence is quenched. When the liposome is degraded or its contents leak through the membrane, ANTS and DPX are diluted in such a way that the quencher's concentration is not sufficient to quench the fluorescence anymore, and the increase in fluorescence is quantitatively interpreted as leakage from liposomes, that is, liposome disintegration (Ellens et al., 1985). ANTS and DPX structures are shown on Figures 3 and 4, respectively.
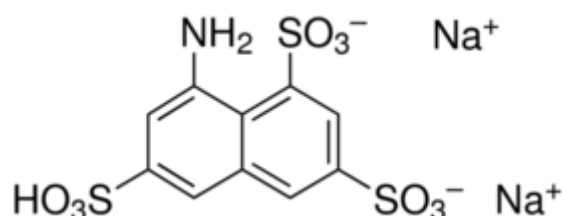

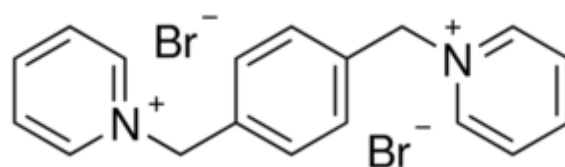Figure 3. ANTS (fluorophore) structure (retrieved from www.sigmaaldrich.com)

Figure 4. DPX (quencher) structure (retrieved from www.sigmaaldrich.com)

3.3. EXPERIMENTAL PROCEDURES

3.3.1. PREPARATION OF PEPTIDE SOLUTIONS

First, two buffers were prepared: 20 mM phosphate + 130 mM sodium chloride, pH=7.4 phosphate-buffered saline (PBS) and 10 mM HEPES (salt-free), pH=7.0 (HEPES$_{SF}$). OP-145, P148 and P276 were available in pre-weighed quantities in small cuvettes. The appropriate buffer, depending on further use, was added to achieve a peptide concentration of 10 mg/ml (OP-145) or 2 mg/ml (P148 and P276). Unless otherwise indicated, all subsequent experiments were performed using all three peptides separately.

3.3.2. PREPARATION OF LIPOSOMES

DPPG and DPPC films used in DSC assays were prepared by first dissolving separately 10 mg each in 1 ml of the appropriate solvent. 100 μl aliquots of these solutions were then transferred to glass vials and the solvent was evaporated under a stream of nitrogen. POPG and POPC films used in CD and size measurements were prepared by dissolving separately 26 mg and 24 mg of lipid, respectively, in 1 ml of the appropriate solvent and subsequent evaporation of the solvent under a stream of nitrogen. Prepared films were kept overnight under vacuum at room temperature and afterwards stored at 4ºC. When ready to use, films were hydrated by adding 1 ml of buffer and vortexing at maximum speed for 1 min, incubated at temperature about 10 ºC above the main transition temperature for the given period of time and vortexed at maximum speed at given intervals for 1 min during the incubation period. Thus prepared liposomal suspensions were allowed to cool and used in further experiments. POPG and POPC liposomes were extruded 15 times through a 0.1 μm pore size membrane filter to gain unilamellar vesicles and size homogeneity. Prior to all further handling the suspensions were briefly vortexed to resuspend the liposomes. The necessary parameters for liposome preparation are given in Table 3. An overview of buffers and types of lipids used in different analytical methods is given in Table 4.

Table 3. Liposomes preparation parameters; RT = room temperature

Lipid	solvent CHCl$_3$:CH$_3$OH (V/V ratio)	incubation temperature (ºC)	incubation period	vortexing intervals
DPPG	9:1	65	1 h	5', 10', 20', 30', 60'
POPG		25 (RT)		
DPPC	2:1	50	2 h	every 15'
POPC		25 (RT)		

Table 4. Lipids and buffers used in different methods. PBS – phosphate-buffered saline; HEPES$_{SF}$ – salt-free HEPES; HEPES$_F$, HEPES$_E$ – see section 3.3.7.1.

Lipid	Technique			
	DSC	DLS	CD	fluorometry
DPPG	PBS	-	-	-
POPG	-	PBS	HEPES$_{SF}$	HEPES$_F$/HEPES$_E$/PBS
DPPC	PBS	-	-	-
POPC	-	PBS	HEPES$_{SF}$	HEPES$_F$/HEPES$_E$/PBS

For DSC analyses DPPG and DPPC were used because they form lipid bilayers that are in the planar gel phase at room temperature. Therefore, by heating them, both pretransition and main transition can be observed. These multilamellar vesicles were prepared both without and with the analysed peptides. Peptides were dissolved in PBS prior to film hydration, with the combined volume of peptide solution and buffer being 1 ml. Different peptide concentrations were prepared, as described in paragraph 3.3.5. In other assays, peptides were added to pre-formed liposomes.

On the other hand, POPG and POPC were used in other experiments because they form bilayers that are fluid already at room temperature, so they mimic real biological membranes in a better fashion.

For leakage assay, 20 mg of lipids or lipid mixtures was used per film. POPC vesicles were prepared both with and without cholesterol (25% molar cholesterol relative to POPC amount;

cholesterol was added during the film formation stage), while POPG vesicles were prepared both with and without peptidoglycan (PGN was added after liposomes formation), both using fluorescent buffer, as described in paragraph 3.3.7.1.

3.3.3. COMPUTER-BASED MODELLING: *IN SILICO* PREDICTION OF PEPTIDE PROPERTIES

The following programmes were used to model OP-145, P148 and P276 and to predict their properties based on their amino acid sequences:

1. PEP-FOLD 2.0 (Shen et al., 2014; Néron B, 2009), used to predict secondary structure and make a 3D model of peptide and
2. WebLab ViewerPro to visualise data generated by PEP-FOLD 2.0.

3.3.4. SECONDARY STRUCTURE DETERMINATION OF PEPTIDES

Secondary structure of peptides alone and in membrane mimetic systems was determined by measuring circular dichroism (CD) in a spectropolarimeter at room temperature. 10 mM HEPES buffer was first measured as a blank in a 0.02 cm quartz cuvette with parameters defined in Table 5. Samples were then measured under same conditions in five groups, peptide concentration being kept constant at 200 μM:

1. Sole peptides in HEPES: OP-145, P148 and P27;
2. Peptides with SDS in 100:1, 25:1 and 6.25:1 SDS:peptide molar ratios;
3. Peptides with DPC in 100:1, 25:1 and 6.25:1 DPC:peptide molar ratios;
4. Peptides with POPG in 100:1, 25:1 and 6.25:1 POPG:peptide molar ratios and
5. Peptides with POPC in 100:1, 25:1 and 6.25:1 POPC:peptide molar ratios.

Samples were measured at 0, 15, 30 and 60 minutes from adding peptides. Blank signal was subtracted from the respective sample spectra. Data obtained from CD measurements was expressed as mean residue molar ellipticity, $[\theta]_{MR}$. Such data files were uploaded to DichroWeb server for analysis in order to determine secondary structure of peptides (Whitmore and Wallace, 2004). CDSSTR programme was used to analyse data (Compton and Johnson, 1986) with Set 4 as a reference set. Results were expressed as percentage of

particular secondary structure in total peptide. Data was processed using JASCO's Spectra Manager and DichroWeb.

Table 5. Parameters for CD scans

Parameter	Value
Sensitivity	Standard (100mdeg)
Start	260 nm
End	180 nm
Data Pitch	0.2 nm
Scanning Mode	Continuous
Scanning Speed	100 nm/min
Response	1 s
Band Width	1.0 nm
Number of Accumulations	3

3.3.5. CALORIMETRIC MEASUREMENTS

DPPG and DPPC multilamellar liposomes suspended in PBS were subjected to differential scanning calorimetry (DSC) analysis in a microcalorimeter, both alone and with different concentration of peptides that were added during the film hydration stage. PBS was used as reference. Scan parameters are shown in Table 6. Sample preparation is specified in Table 7. After measurements, thermogram baseline was corrected and normalised to the mass of phospholipid. The phase transition temperature was defined as the temperature at the peak maximum. Phase transition enthalpies were calculated by integration of the peak areas. Data was processed using Origin software.

Table 6. Parameters for DSC scans

Number of Scans	6 (3 heating and 3 cooling)
Starting Temperature	10 ºC
Final Temperature	55 ºC
Scan Rate	30 ºC/min
Prescan Equilibration	15 min
Postscan Thermostat	0 min

Table 7. Samples analysed with DSC.

Sample (V=1 ml)	lipid concentration (mg/ml)	lipid concentration (μmol/ml)	peptide concentration (μmol/ml)	lipid-to-peptide molar ratio
DPPG pure			-	-
DPPG + OP-145 2%	1	1.34	0.027	50:1
DPPG + OP-145 4%			0.054	25:1
DPPG + P148 1%			0.013	100:1
DPPG + P148 2%			0.027	50:1
DPPG + P148 4%	1	1.34	0.054	25:1
DPPG + P276 1%			0.013	100:1
DPPG + P276 2%			0.027	50:1
DPPG + P276 4%			0.054	25:1
DPPC pure			-	-
DPPC + OP-145 4%	1	1.36	0.054	25:1
DPPC + P148 4%			0.054	25:1
DPPC + P276 4%			0.054	25:1

3.3.6. SIZE MEASUREMENT OF LIPOSOMES

Liposomes size was measured using dynamic light scattering (DLS) with Zetasizer Nano at automatic mode. POPG and POPC liposomes in concentrations of 1 mg/ml of PBS buffer were extruded through 0.1 µm membranes prior to measurement to reduce them to unilamellar vesicles. 1 ml of PBS filtered through a 0.1 µm filter was put in a quartz cuvette. 50 µl of liposome suspension, with or without peptide, was added to the cuvette, mixed by pulling the liquid in and out of the pipette and the sample was measured. Both types of vesicles were analysed alone and with all three peptides at different concentrations (100:1, 25:1 and 6.25:1 lipid:peptide molar ratios). Measurements were made at 0, 15, 30 and 60 minutes from adding peptides at room temperature.

3.3.7. VESICLE LEAKAGE ASSAY - FLUOROMETRY

A modified assay by Ellens et al. was performed to establish the degree of vesicle leakage induced by the peptides (Ellens et al., 1985).

3.3.7.1. PREPARATION OF FLUORESCENT DYE-CONTAINING VESICLES

20 mg POPC, POPC/cholesterol and POPG films were hydrated with 1 ml of 12.5 mM ANTS, 45 mM DPX, 68 mM sodium chloride, 10 mM HEPES, pH=7.4 buffer (HEPES$_F$) and incubated for 1.5 h at 30 ºC with intermittent vortexing at 5, 10, 25, 40, 55, 75 and 85 minutes from start. After cooling to room temperature fluorescent dye-containing liposomes were extruded 15 times through a 0.1 µm pore size membrane filter to achieve unilamellarity and subjected to gel filtration (size-exclusion chromatography – stationary phase: Sephadex™ G-75; eluent: 10 mM HEPES, 140 mM sodium chloride, 1 mM EDTA, pH=7.4 buffer (HEPES$_E$)). First 40 drops were discarded; subsequently, every 10 drops were separately collected into fractions. These fractions were subjected to a Cary Eclipse fluorescence spectrophotometer with excitation at 360 nm and emission at 530 nm to determine which ones have the highest concentration of liposomes. The most adequate fractions were combined and used thereafter. Exact phospholipid concentration was determined by phosphate analysis (Bartlett, 1959).

3.3.7.2. FLUORESCENCE MEASUREMENT – VESICLE LEAKAGE ASSAY

All measurements were performed at 37 ºC with magnetic stirring at constant speed. Required volume of liposome sample was added into 2 ml of PBS in a quartz cuvette to achieve a final lipid concentration of 50 µM and measured using an excitation wavelength of 360 nm, emission wavelength of 530 nm and a 10 nm slit width for both excitation and emission monochromators to determine initial fluorescence. Next, increasing concentrations of different peptides were added and fluorescence was measured after 15 min of incubation. At the end, 10 µl of 10% Triton™ X-100 detergent was added to determine total fluorescence. Peptide concentrations are specified in Table 8. Fluorometry results were expressed in arbitrary units. To show the degree of fluorophore leakage from vesicles, data was presented

in terms of fluorescence intensity and expressed as percentage according to the following formula (Zweytick et al., 2011):

$$I_F = \frac{F - F_0}{F_{max} - F_0} \cdot 100\%$$

where F is the measured fluorescence, F_0 is initial fluorescence (without peptides) and F_{max} is total fluorescence after liposome disintegration with detergent.

To prepare POPG vesicles with peptidoglycan, PGN was first dissolved in PBS, heating it for 15 min at 95 ºC, to a concentration of 0.5 mg/ml. Heating is used to deactivate proteases that have previously been found in commercial PGN samples, so as not to degrade the peptides. 4 µl of this solution was added together with the required volume of POPG sample into 2 ml of PBS to a final concentration of 50 µM POPG and 0.01% weight PGN. It was then proceeded as described earlier.

Table 8. Peptide concentrations in leakage assays. (*only certain measurements)

Peptide concentration (µM)	Peptide conc. relative to lipid (% molar)
0	0
0.0625	0.125%
0.125	0.25%
0.25	0.5%
0.5	1%
1	2%
2	4%
4	8%
8*	16%*

3.3.7.3. VESICLE LEAKAGE ASSAY IN PRESENCE OF BOVINE SERUM

POPC and POPG fluorescent dye-containing vesicles were subjected to a leakage assay in the presence of selected concentrations of peptides and two different concentrations of bovine serum: 10% and 25% (V/V), whereas the total volume was kept at 2 ml. Procedure was as described in section 3.2.7.2. Peptide concentrations are given as follows:

1. OP-145 was analysed with POPC and POPG in the presence of 10% and 25% serum through all concentrations as specified in Table 8;
2. P148 was analysed with POPC in the presence of 10% and 25% serum through all concentrations as specified in Table 8. With POPG, only concentrations of 0.0625, 0.5 and 4 μM were analysed in the presence of 10% serum as it was shown that bovine serum alone causes near complete leakage from POPG vesicles.
3. P276 was not analysed.

3.3.7.4. VESICLE LEAKAGE IN PRESENCE OF BOVINE SERUM ALBUMIN

In order to examine the effect of bovine serum albumin (BSA) on membrane permeability properties of AMPs, leakage experiments were performed with BSA concentrations ranging from 0 to 9 % molar on POPG and POPC vesicles. Fluorescent dye-containing POPG and POPC vesicles were separately diluted in a quartz cuvette containing 1.85 ml of PBS to a total concentration of 50 μM and initial fluorescence was measured. Increasing amounts of BSA standard were consecutively added and fluorescence measured when the signal had been stabilised. In the end 10 μl of 10% Triton™ X-100 was added to determine total fluorescence. BSA concentrations are given in Table 9.

Table 9. BSA concentration in fluorometry assays

BSA concentration (μM)	peptide conc. relative to lipid (% molar)
0	0
0.0625	0.125%
0.125	0.25%
0.25	0.5%
0.5	1%
1	2%
2	4%
4	8%
4.5	9%

3.3.8. PEPTIDE-LIPID AFFINITY ASSAY

Fluorescent dye-containing POPG vesicles were mixed at the same concentration with non-dye containing POPC unilamellar vesicles and vice-versa and added into 2 ml PBS in a quartz cuvette to a total lipid concentration of 100 µM. It was then processed as described in section 3.2.7.2. Peptide concentrations are given in Table 10.

Table 10. Peptide concentration in peptide-lipid affinity leakage assays

Peptide concentration (µM)	peptide conc. relative to lipid (% molar)
0	0
0.0625	0.0625%
0.125	0.125%
0.25	0.25%
0.5	0.5%
1	1%
2	2%
4	4%

4. RESULTS

4.1. *IN SILICO* STRUCTURAL PROPERTIES OF AMPS

4.1.1. OP-145

Secondary structure predicted by PEP-FOLD 2.0 for OP-145 was mostly alpha helical as depicted on Figures 5-7. Hydrophobic residues of the predicted alpha helix are segregated on the one side and hydrophilic regions on the other side, forming an ideal amphipathic helix (Figure 8).
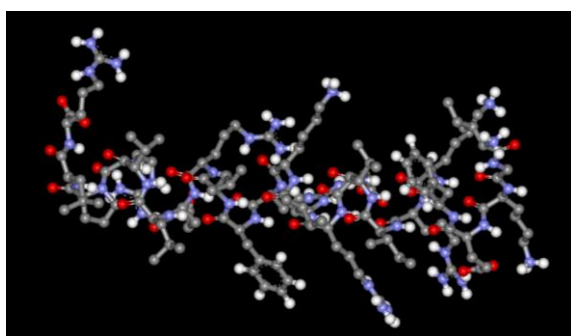

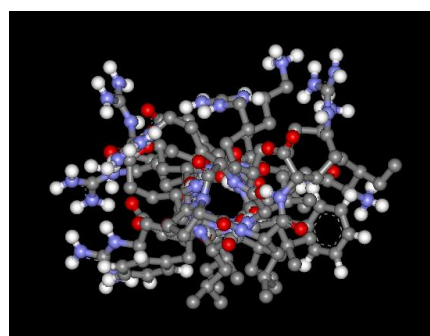Figure 5. Side view of OP-145 secondary structure computer model.

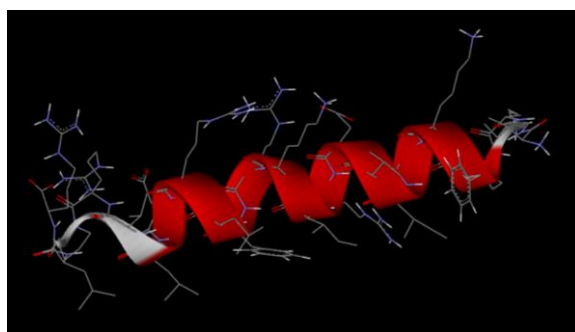Figure 6. OP-145 alpha helix viewed along the main axis (N to C terminus).

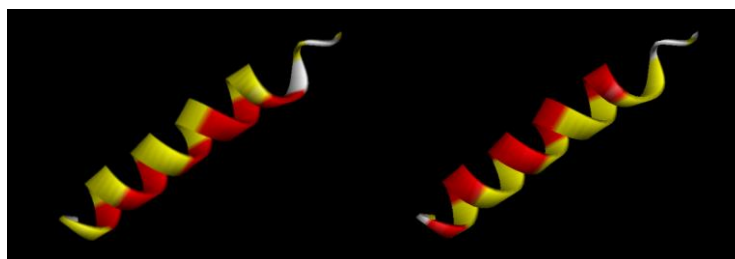Figure 7. OP-145 model alpha helix backbone displayed as a ribbon.

Figure 8. Hydrophilic (left) and hydrophobic (right) domains of OP-145 model alpha helix (in yellow).

4.1.2. P148

Secondary structure predicted by PEP-FOLD 2.0 for P148 was slightly less alpha helical than the one of OP-145 (Figure 9), however hydrophilic and hydrophobic domains were located opposite one another to form an amphipathic helix, as with OP-145 (Figure 10). In addition, P148 exhibit large non-flexible tail on C terminus which does not fold into a helix.
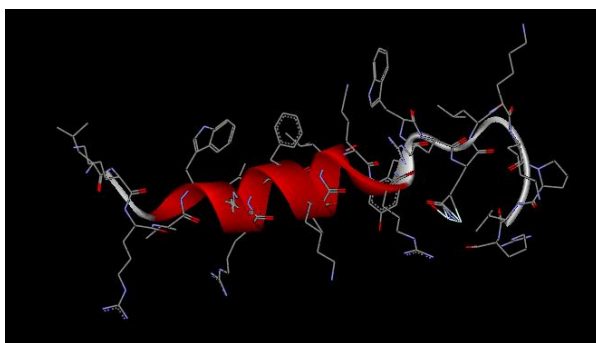

Figure 9. Computer-generated model of P148
secondary structure. Alpha helix shown as red ribbon.

Figure 10. P148 hydrophilic (left) and hydrophobic (right) alpha helix domains (in yellow).

4.1.3. P276

Secondary structure predicted by PEP-FOLD 2.0 for P276 was very similar to P148 (Figure 11), both in helicity and hydropathic domains (Figure 12) again showing an unordered C-terminus tail.
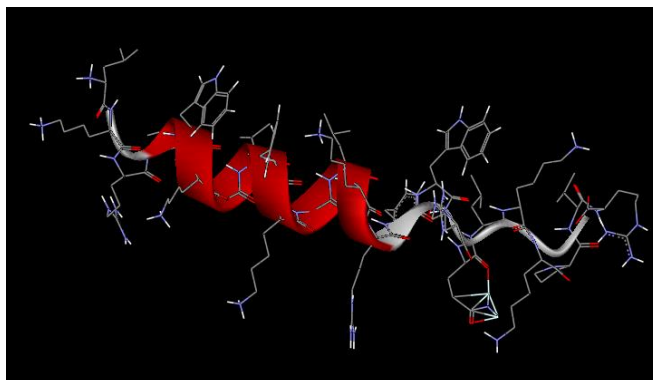

Figure 11. Computer-generated model of P276 secondary structure. Alpha helix shown as red ribbon.
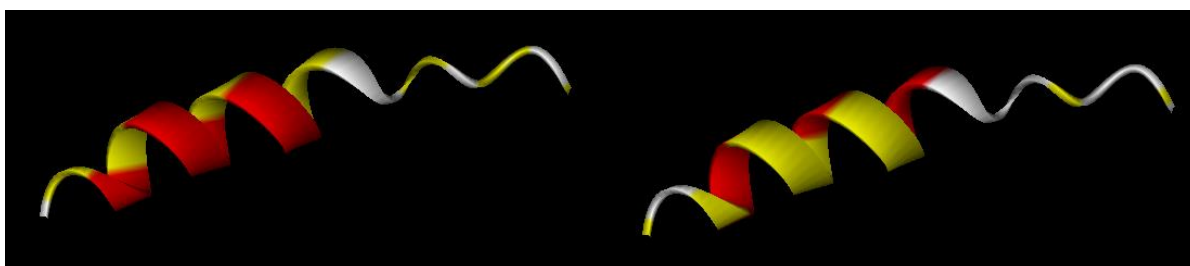

Figure 12. P276 hydrophilic (left) and hydrophobic (right) alpha helix domains (in yellow).

4.2. SECONDARY STRUCTURE DETERMINATION OF PEPTIDES

In order to validate the data from prediction analysis CD spectroscopy has been performed. CD spectra of analysed AMPs have been recorded in presence of HEPES buffer, negatively charged SDS micelles and POPG vesicles as well as zwitterionic DPC micelles POPC vesicles mimicking bacterial and mammalian membrane, respectively. In addition, time-dependent measurements between 0 and 60 min upon incubation with membrane mimics have been performed in order to follow secondary structure formation/development on lipid membranes.

4.2.1. OP-145

CD measurements and subsequent data processing have shown that OP-145 takes a mostly alpha helical secondary structure both in buffer and in contact with POPC and DPC that seems to be stable over time (Figures 13, 16 and 17). On the other hand, in interaction with POPG and SDS, the alpha helicity of the secondary structure of OP-145 diminishes over time and with the increase of the peptide's concentration, falling from around 60-80% alpha helix in a lipid to peptide ratio of 100:1 to around 10% at 60 minutes at a ratio of 6.25:1 (Figures 14 and 15).
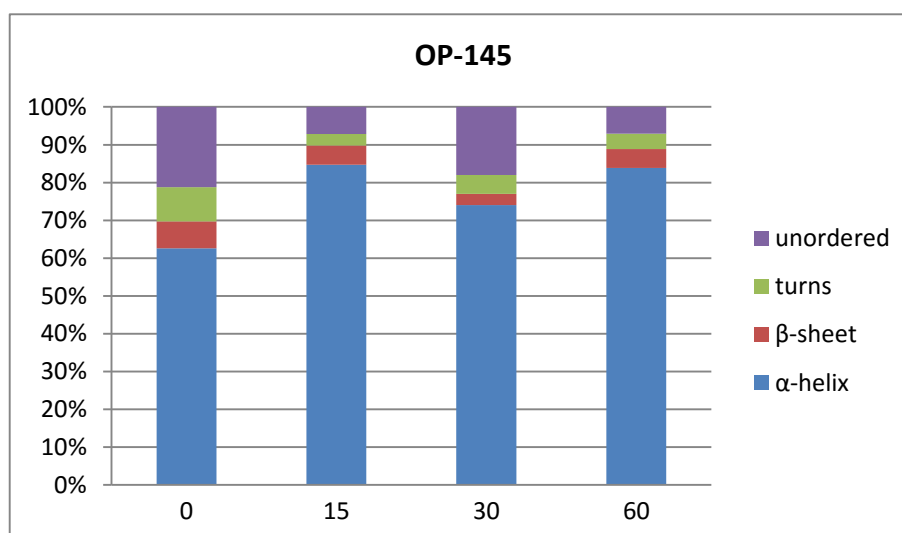

Figure 13. OP-145 time-dependent secondary structure in buffer. Time is expressed in min.
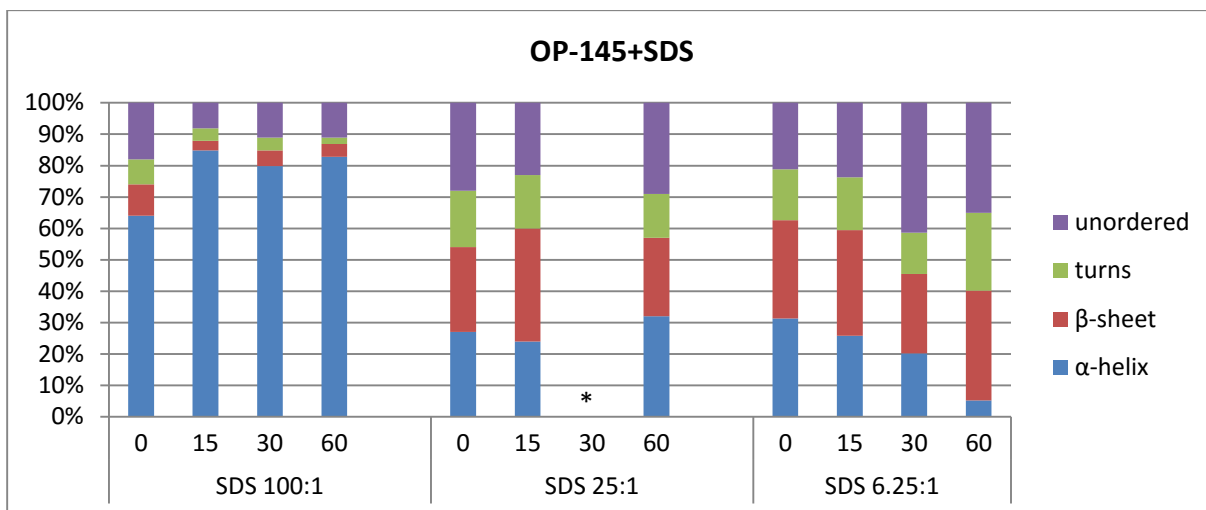
Figure 14. OP-145 time-dependent secondary structure in interaction with SDS at different molar ratios. Time is expressed in minutes. (*data is lacking)
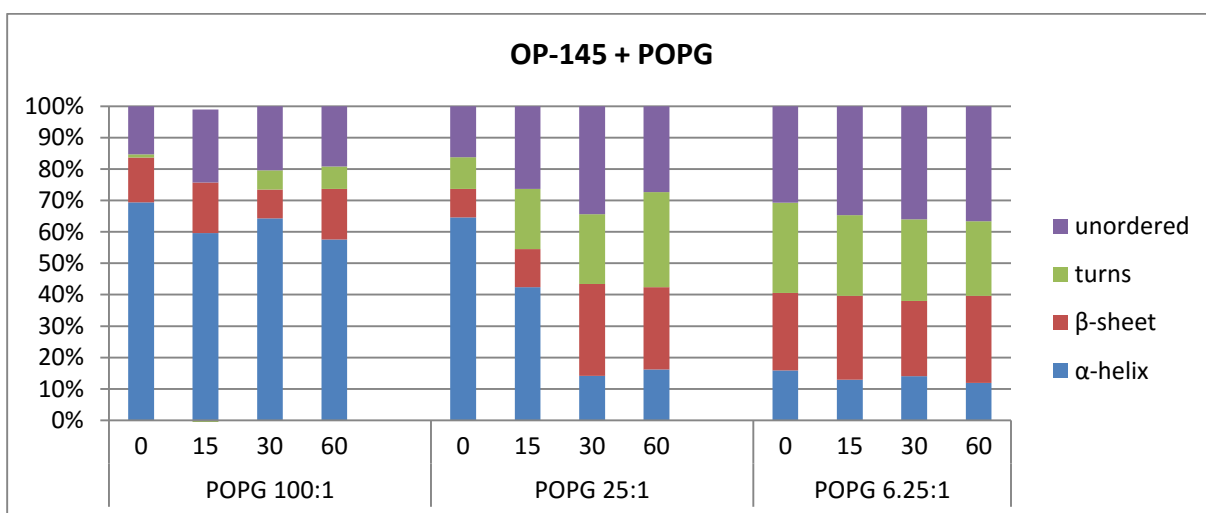

Figure 15. OP-145 time-dependent secondary structure in interaction with POPG at different molar ratios. Time is expressed in minutes.
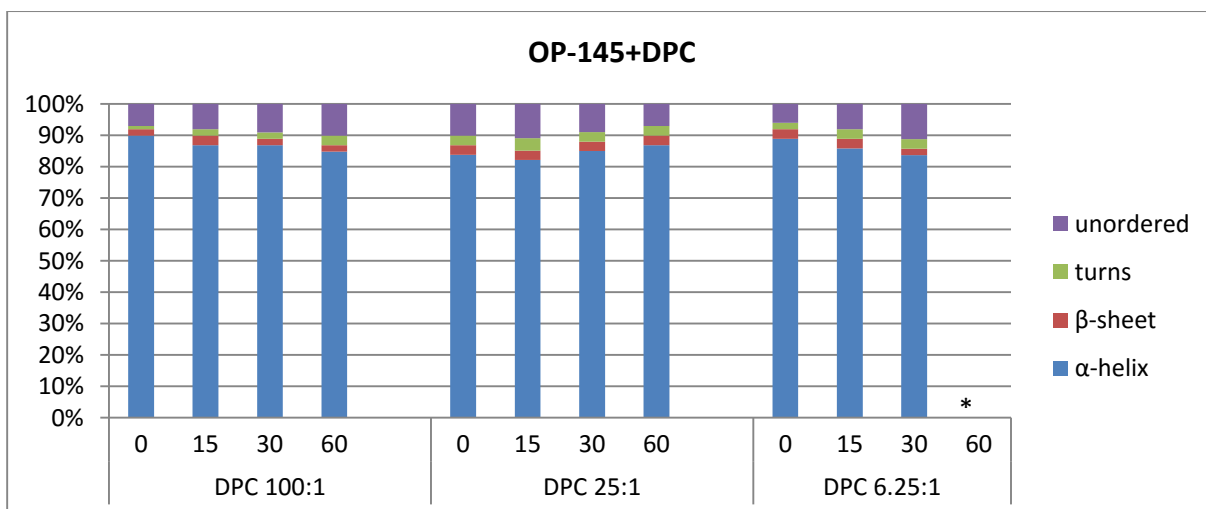

Figure 16. OP-145 time-dependent secondary structure in interaction with DPC at different molar ratios. Time is expressed in minutes. (*data is lacking)
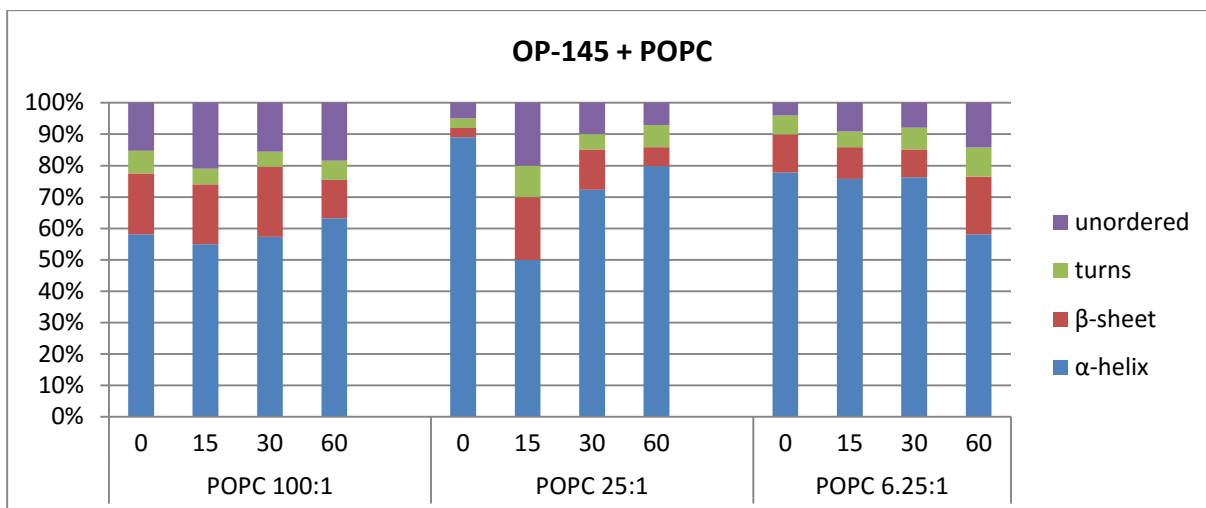
Figure 17. OP-145 time-dependent secondary structure in interaction with POPC at different molar ratios. Time is expressed in minutes.

4.2.2. P148

Results show that P148 does not take an alpha helical secondary structure when measured in buffer (Figure 18). However, in contact with both prokaryotic and eukaryotic model membranes, at lower peptide concentrations, it has a rather large proportion of alpha helix in its secondary structure. With an increase in peptide concentration, the portion of alpha helix diminishes, especially in contact with POPC membranes (Figures 19-22).

Figure 18. P148 time-dependent secondary structure in buffer. Time is expressed in min.

Figure 19. OP-145 time-dependent secondary structure in interaction with SDS at different molar ratios. Time is expressed in minutes.

Figure 20. P148 time-dependent secondary structure in interaction with POPG at different molar ratios. Time is expressed in minutes.

Figure 21. OP-145 time-dependent secondary structure in interaction with DPC at different molar ratios. Time is expressed in minutes. (*data is lacking)
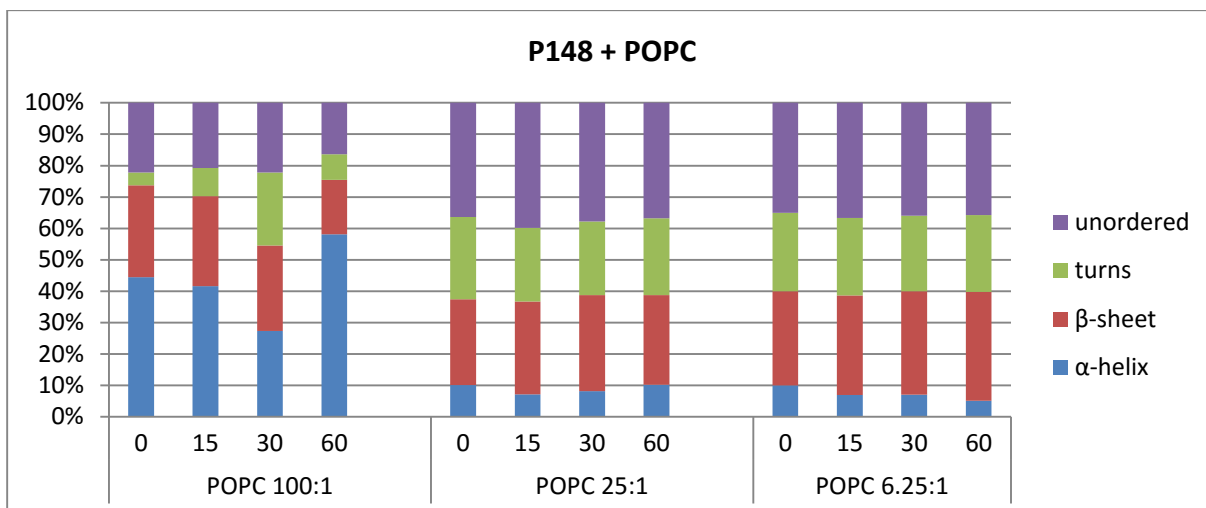
Figure 22. P148 time-dependent secondary structure in interaction with POPC at different molar ratios. Time is expressed in minutes.

4.2.3 P276

Measurement results show that P276 does not take an alpha helical conformation in buffer (Figure 23). The proportion of alpha helix is quite high in SDS and DPC micelles, around 60% (Figures 24 and 26), while in contact with POPG and POPC membranes secondary structure again seems to diminish with the increase of peptide's concentration, especially with POPC (Figures 25 and 27). However, results seems to be unstable over time, so it cannot be estimated how precise they are, especially for POPG.
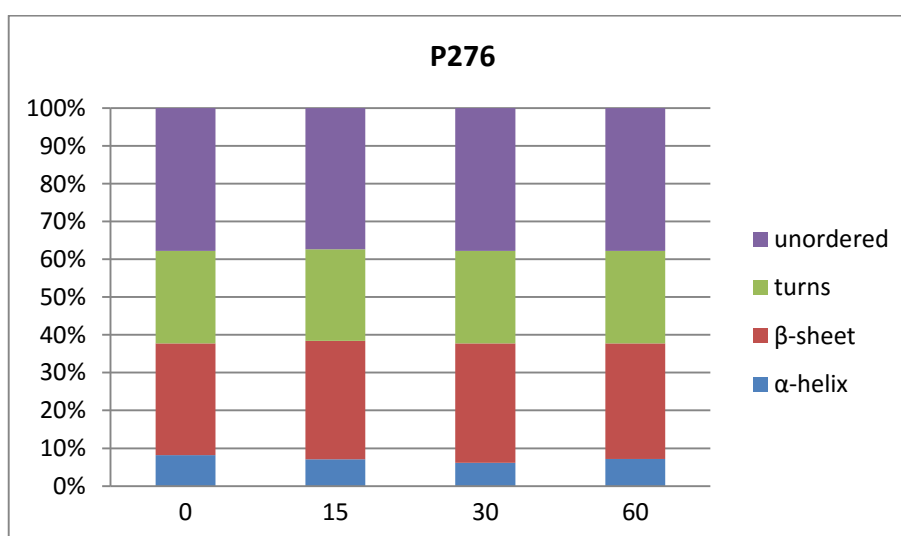
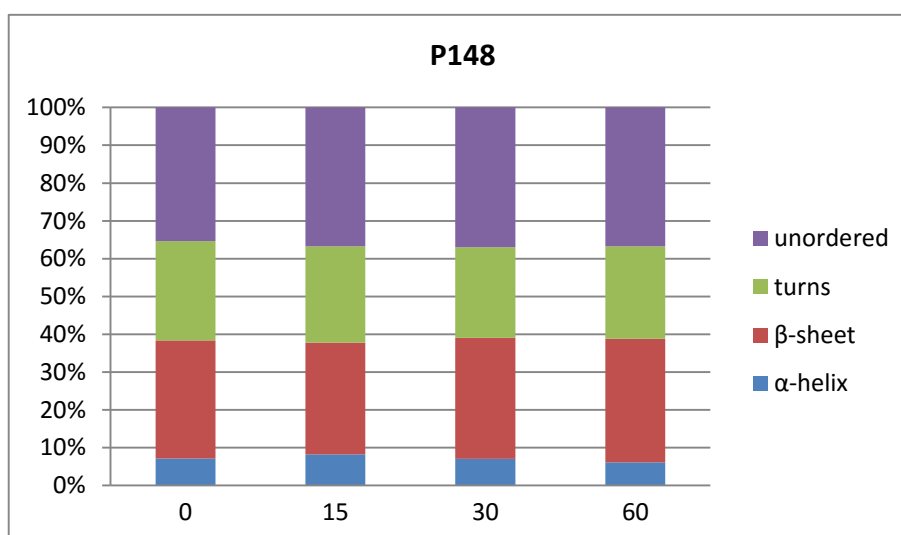
Figure 23. P276 time-dependent secondary structure in buffer. Time is expressed in min.

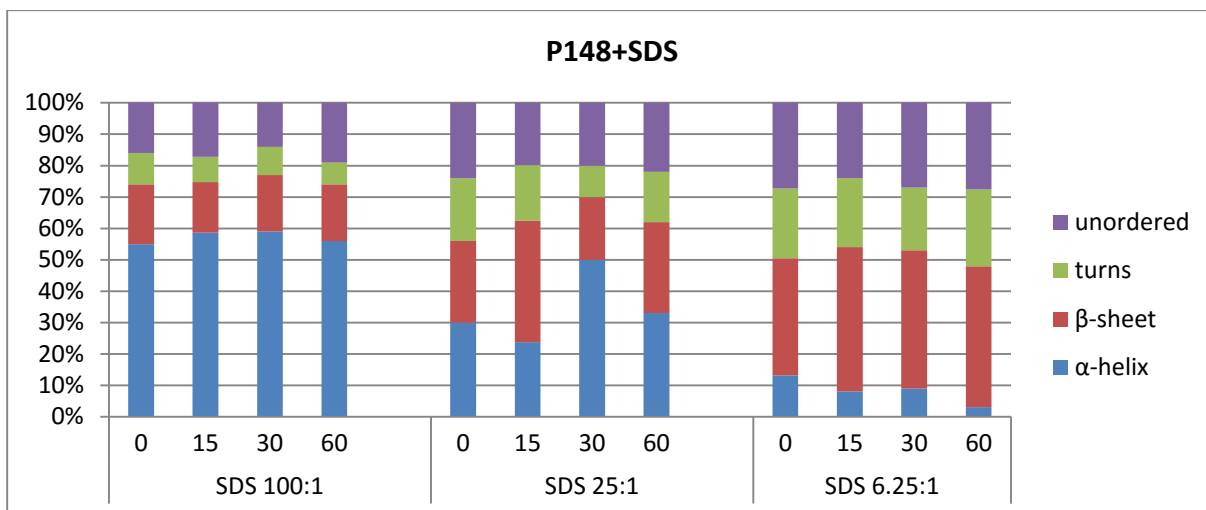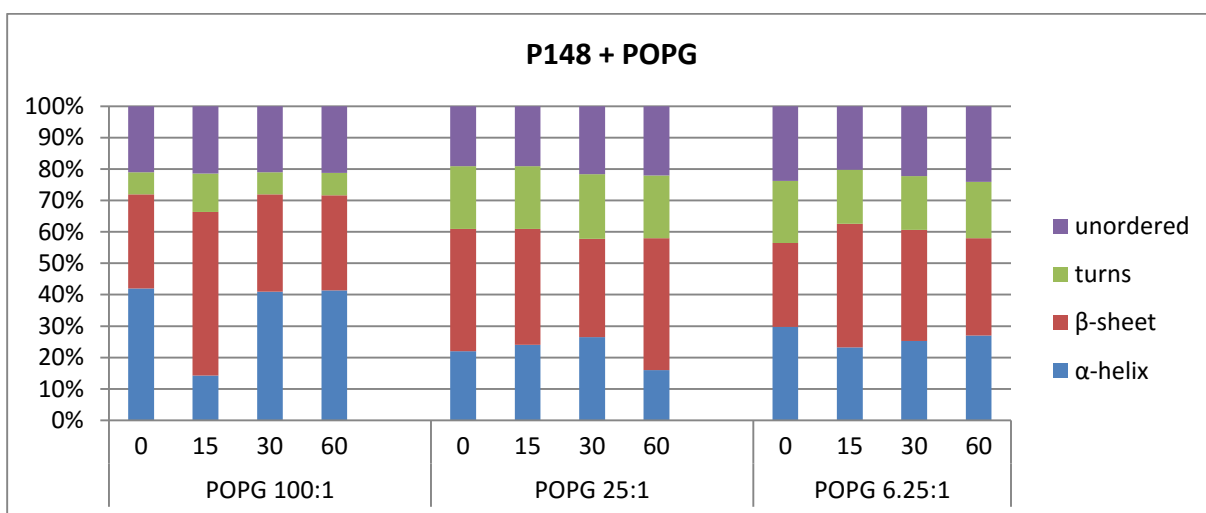Figure 24. P276 time-dependent secondary structure in interaction with SDS at different molar ratios. Time is expressed in minutes.

Figure 25. P276 time-dependent secondary structure in interaction with POPG at different molar ratios. Time is expressed in minutes.
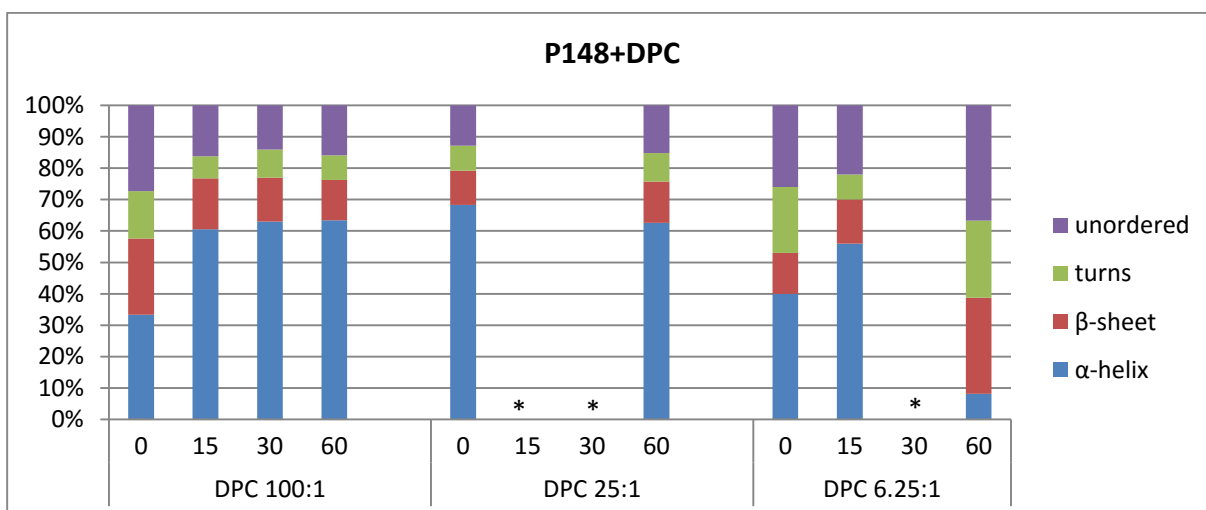

Figure 26. P276 time-dependent secondary structure in interaction with DPC at different molar ratios. Time is expressed in minutes. (*data is lacking)
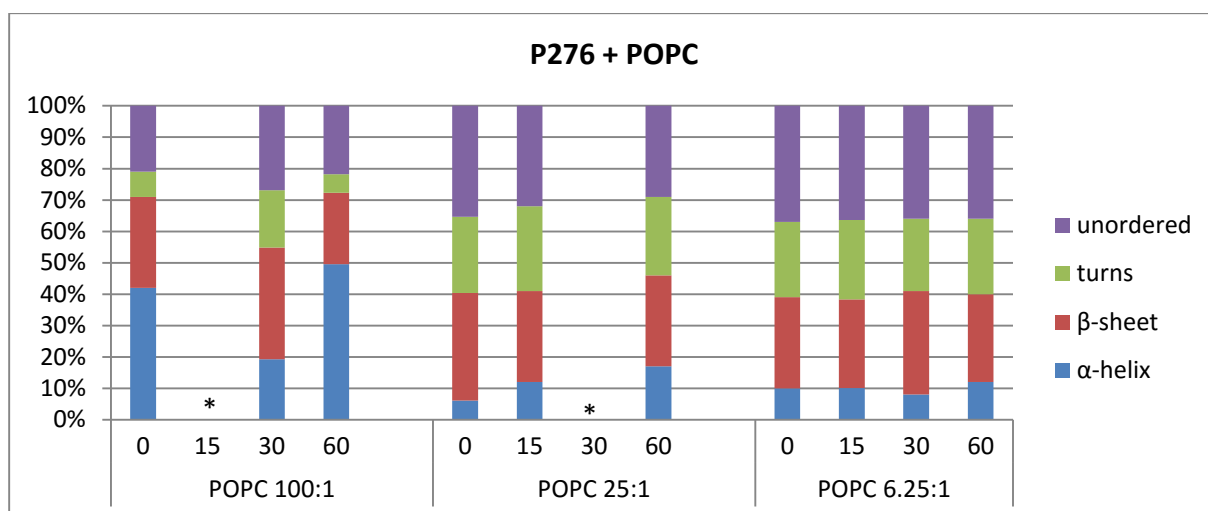
Figure 27. P276 time-dependent secondary structure in interaction with POPC at different molar ratios. Time is expressed in minutes. (*data is lacking)

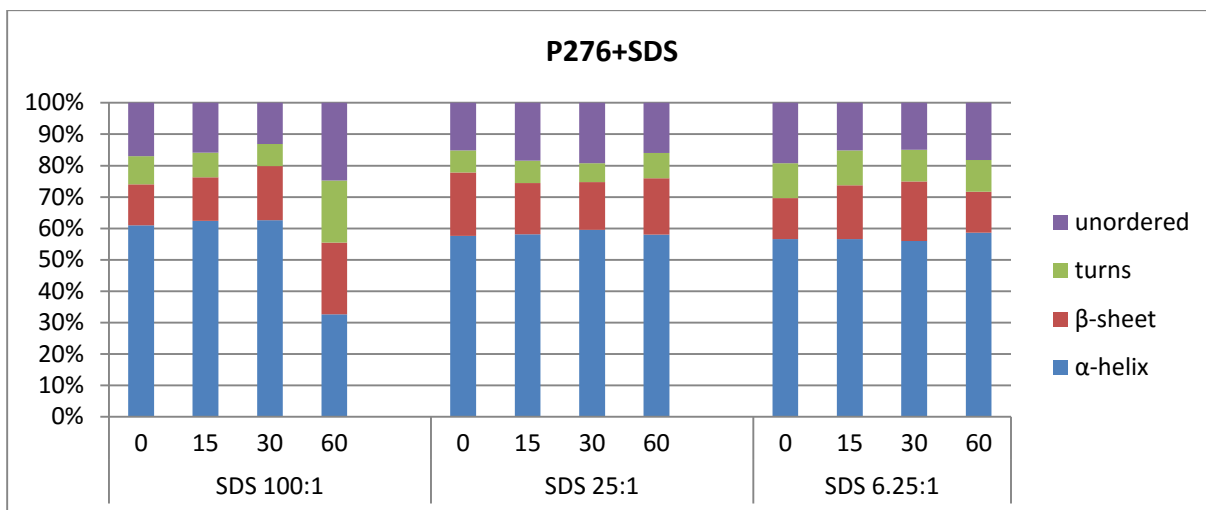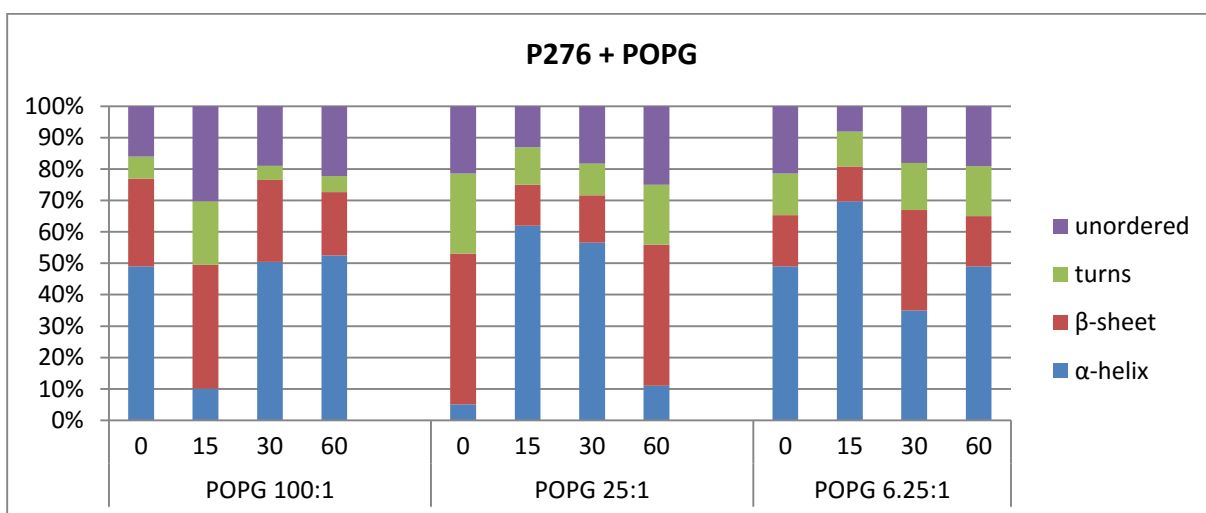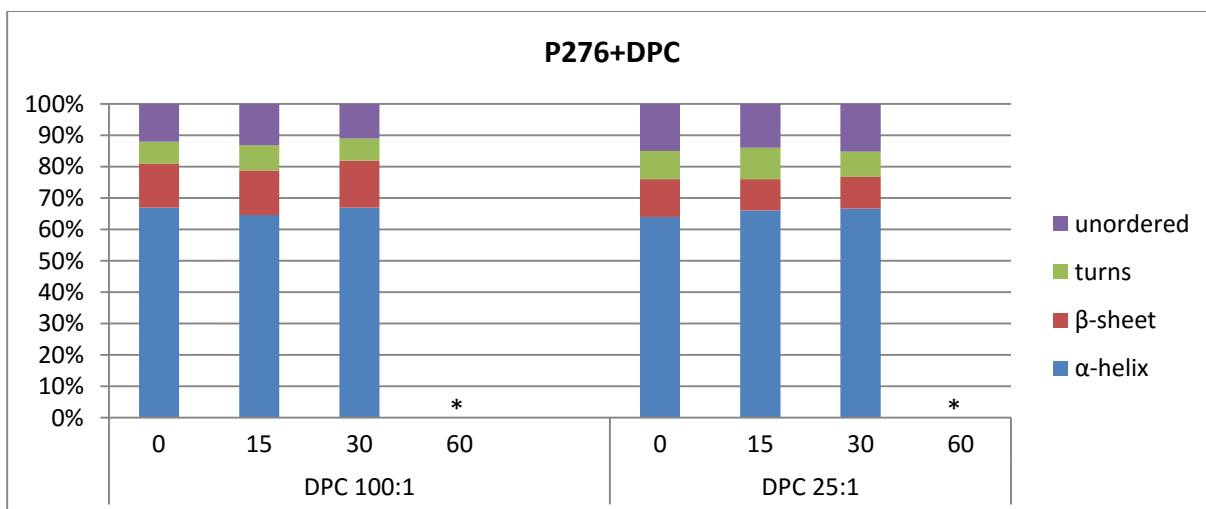## 4.3. SIZE MEASUREMENT OF LIPOSOMES

Dynamic light scattering measurements were performed to measure the size of liposomes in contact with different concentrations of peptides in order to determine the impact of vesicle size on secondary structure of peptides and to check the stability of liposomes over time. Results are shown in Figures 28 and 29 as POPG and POPC liposomes size dependent on peptide concentration and time. Data obtained from dynamic light scattering measurements was expressed as Z-average diameter.

The size of POPG liposomes in interaction with OP-145 has increased nearly three-fold over time with the increase of peptide concentration, from around 150 nm to about 450 nm. Further, size of POPG liposomes in combination with P148 and P276 does not change with the addition of 1% peptide. It then seems to increase mildly, roughly by 15%, with peptide concentration 4 times higher than the starting one; further addition of peptide to a concentration 16 times higher than the starting one seems to decrease the size slightly by around 10% from the pure liposome size.

The size of POPC liposomes seems to be stable regardless of peptide concentration and passage of time. Pure liposome sizes of both POPG and POPC have shown to be stable over time and are given for reference.

Polydispersity indices (PDIs) that show the width of size distribution are shown in Tables 11 and 12. Values between 0.1 and 0.4, such as the ones obtained from these measurements, indicate an intermediate or moderate size distribution (www.malvern.com).
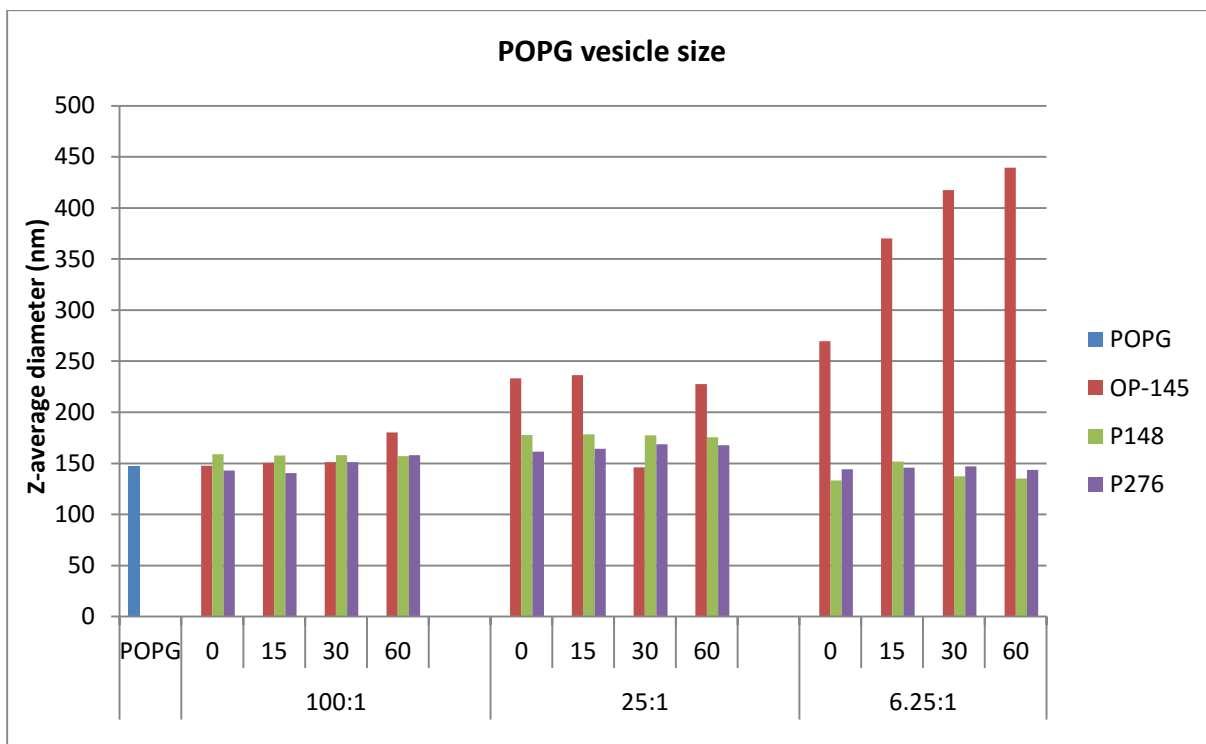
Figure 28. POPG liposomes size dependent on peptides concentration (given as lipid:peptide molar ratio) and time (given in min)
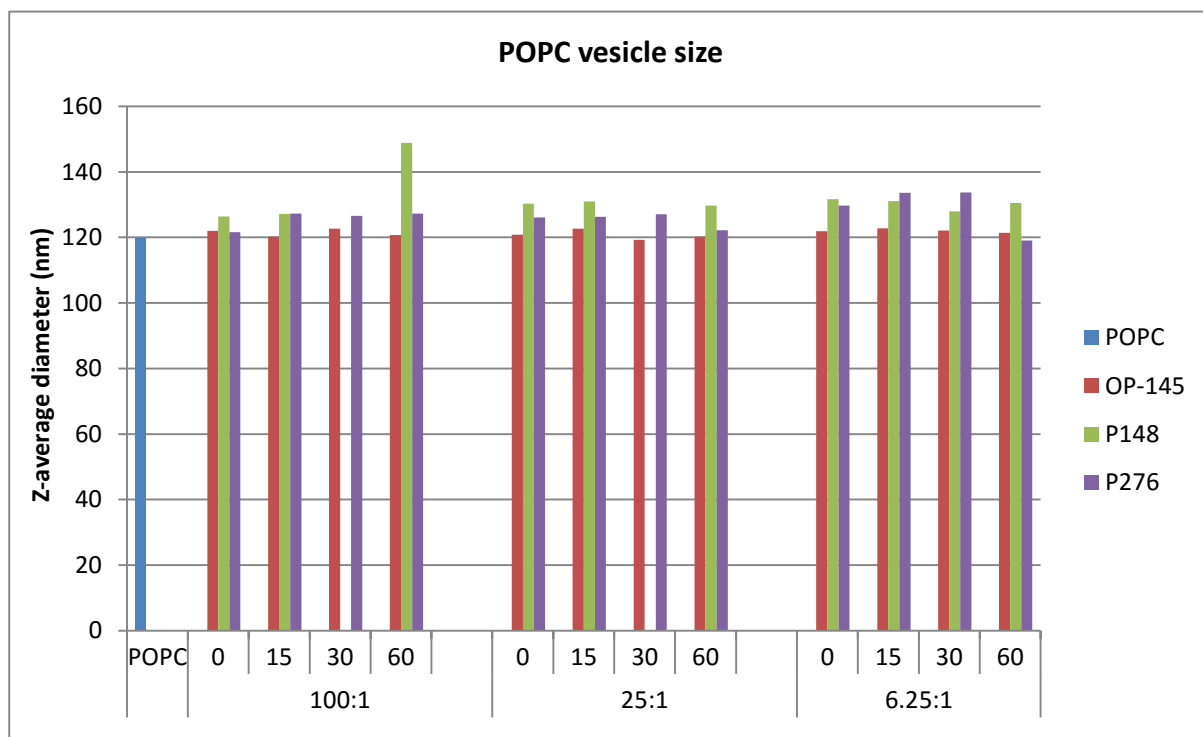
Figure 29. POPC liposomes size dependent on peptides concentration (given as lipid:peptide molar ratio) and time (given in min)

Table 11. Particle size polydispersity indices (PDIs) of POPG vesicles.

POPG pure	0.087	PDI		
	Time (min)	OP-145	P148	P276
100:1	0	0.205	0.215	0.168
	15	0.223	0.206	0.212
	30	0.166	0.204	0.241
	60	0.365	0.213	0.244
25:1	0	0.332	0.147	0.138
	15	0.271	0.127	0.158
	30	0.206	0.138	0.141
	60	0.34	0.161	0.143
6.25:1	0	0.276	0.126	0.123
	15	0.176	0.198	0.164
	30	0.171	0.136	0.139
	60	0.203	0.144	0.138

Table 12. Particle size polydispersity indices (PDIs) of POPC vesicles.

POPC pure	0.059	PDI		
	Time (min)	OP-145	P148	P276
100:1	0	0.07	0.068	0.144
	15	0.089	0.049	0.051
	30	0.066	-	0.052
	60	0.053	0.195	0.052
25:1	0	0.063	0.079	0.09
	15	0.039	0.086	0.157
	30	0.064	-	0.076
	60	0.027	0.021	0.041
6.25:1	0	0.051	0.077	0.109
	15	0.027	0.038	0.1
	30	0.061	0.078	0.101
	60	0.045	0.059	0.089

4.4. CALORIMETRIC MEASUREMENTS: INTERACTION OF AMPS WITH BACTERIAL AND MAMMALIAN MODEL MEMBRANES

In order to assess the interaction of AMPs with model membranes, differential scanning calorimetry measurements were performed of liposomes composed of DPPG and DPPC. Both phospholipids have characteristic phase transition behaviour (Figure 30 and 31) that can be described by typical parameters, e.g. phase transition temperature, transition enthalpy and half width summarized in Table 13 and 14.

Upon interaction of OP-145 with DPPG, the phase transition temperature of DPPG increased in heating scans by about 1 °C. DPPG transition temperatures in contact with other peptides at different concentrations are largely unaffected, except for P276 at a 25:1 lipid:P276 ratio which shifts the transition towards a lower value by 0.7 °C. Transition enthalpies are to a great extent unaffected; the highest concentration of P148 (25:1 lipid:peptide ratio) stands out as the only concentration at which enthalpy has decreased by more than 10% from the pure lipid value. Pretransitions have completely disappeared in lipid:peptide ratios of 50:1 and lower (meaning higher concentration of peptides).

On the other hand, cooling scans are showing strong shifts in transition temperatures of DPPG at high peptide concentration, with OP-145 and P276 causing mutually comparable shifts of nearly 2 °C towards lower values and P148 showing a weaker, but still highly prominent shift of 0.7 °C. Lower concentrations seem to cause no effect on the phase transition temperature, except the 100:1 lipid:P148 ratio, which causes a peak splitting. This indicates a formation of two different domains, a peptide-rich DPPG domain and peptide-poor domain. Enthalpies also seem to differ from the reference value, but it cannot be assessed if those differences are of any significance.

Figure 30. Heating DSC thermograms of DPPG combined with peptides in different molar ratios. *pretransition

Table 13. Specific enthalpies and transition temperatures of DPPG vesicles combined with peptides in different molar ratios (heating scans).

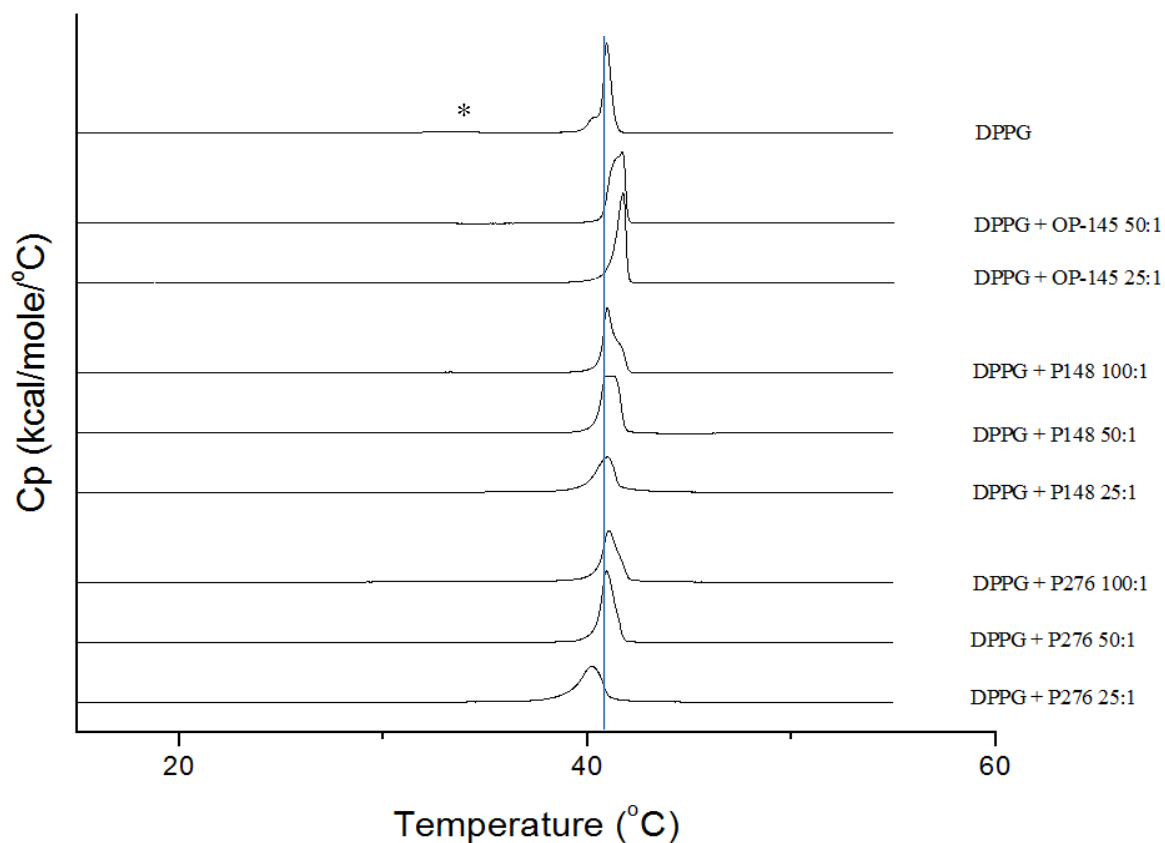|		PRETRANSITION			MAIN TRANSITION	
	Tm (°C)	ΔHm_{pre} (kcal/mol)	$\Delta T1/2$	Tm (°C)	ΔHm (kcal/mol)	$\Delta T1/2$
pure DPPG	33.6	1.5	3.90	40.9	10.0	0.42
OP-145 50:1	-	-	-	41.7	10.3	0.87
OP-145 25:1	-	-	-	41.7	9.8	0.52
P148 100:1	33.3	0.4	2.59	41.0	9.2	0.69
P148 50:1	-	-	-	41.0	10.4	1.04
P148 25:1	-	-	-	41.0	8.8	1.05
P276 100:1	32.6	0.5	5.08	41.0	9.6	0.90
P276 50:1	-	-	-	40.9	9.6	0.73
P276 25:1	-	-	-	40.2	9.7	1.30
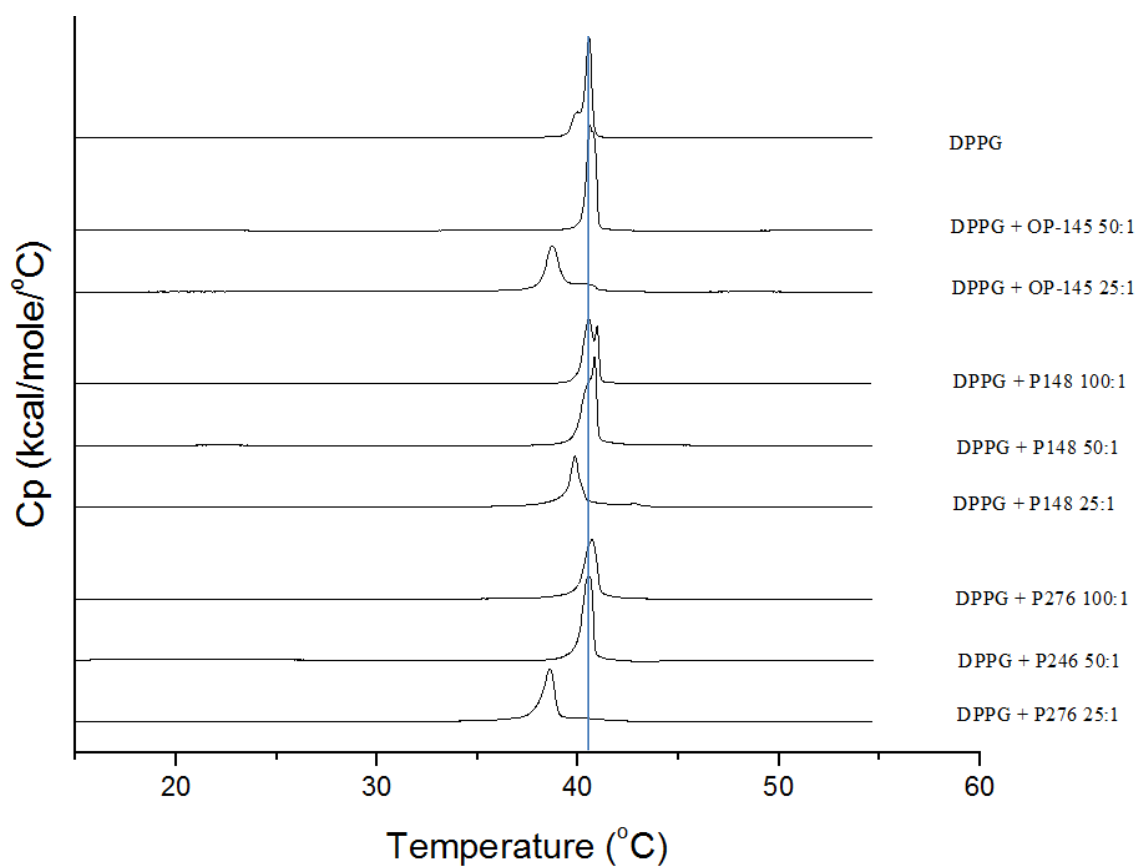
Figure 31. Cooling DSC thermograms of DPPG combined with peptides in different molar ratios.

Table 14. Specific enthalpies and transition temperatures of DPPG vesicles combined with peptides in different molar ratios (cooling scans).

	MAIN TRANSITION		
	Tm (°C)	ΔHm (kcal/mol)	ΔT1/2
pure DPPG	40.5	8.6	0.35
OP-145 50:1	40.6	10.2	0.53
OP-145 25:1	38.7	9.1	0.75
P148 100:1	40.5	6.3	0.59
P148 50:1	40.8	11.2	0.70
P148 25:1	39.8	7.6	0.53
P276 100:1	40.7	9.0	0.72
P276 50:1	40.6	8.5	0.58
P276 25:1	38.6	9.3	0.68

DPPC thermograms show a strong influence of peptides on the thermotropic phase behaviour of DPPC (Figures 32 and 33 and Tables 15 and 16). All three peptides, at the single analysed concentration, i.e. ratio of 25:1 lipid:peptide, cause the main transition peak to split into three smaller, but much broader peaks (with much higher $\Delta T_{1/2}$ values), one below, one at and the third above the DPPC main transition temperature. As with DPPG, the pretransition peak disappears in interaction with all three peptides. The cooling scans show quite a similar profile. In both cases, transition enthalpies are significantly lower, more pronounced in the case of addition of P148 and P276 than for OP-145.

Figure 32. Heating DSC thermograms of DPPC combined with peptides in molar ratio of 25:1. +pretransition, *peptide rich domain, #peptide poor domain

Table 15. Specific enthalpies and transition temperatures of DPPC vesicles combined with peptides in molar ratio of 25:1 (heating scans). *peptide rich domain, #peptide poor domain

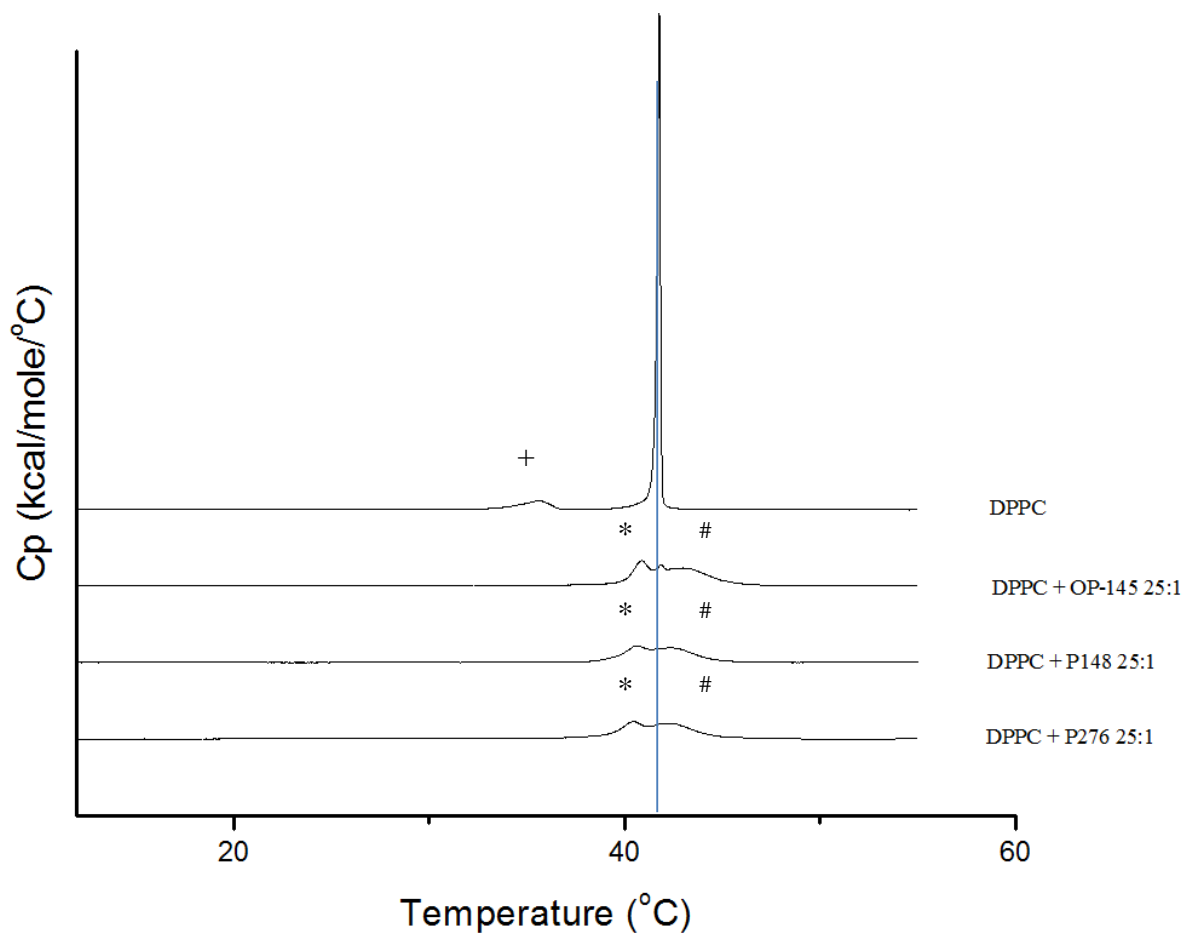|		PRETRANSITION			MAIN TRANSITION		
	Tm (°C)	ΔHm_{pre} (kcal/mol)	$\Delta T1/2$	Tm (°C)	ΔHm (kcal/mol)	$\Delta T1/2$	
DPPC	35.7	1.1	1.92	41.8	8.2	0.18	
OP-145 25:1	-	-	-	40.9	2.1	1.10	*
			-->	41.9	0.9	0.73	
			-->	43.0	2.9	2.29	#
P148 25:1	-	-	-	40.6	1.8	1.47	*
			-->	42.3	2.4	2.36	#
P276 25:1	-	-	-	40.5	1.9	1.49	*
			-->	42.3	2.6	2.54	#
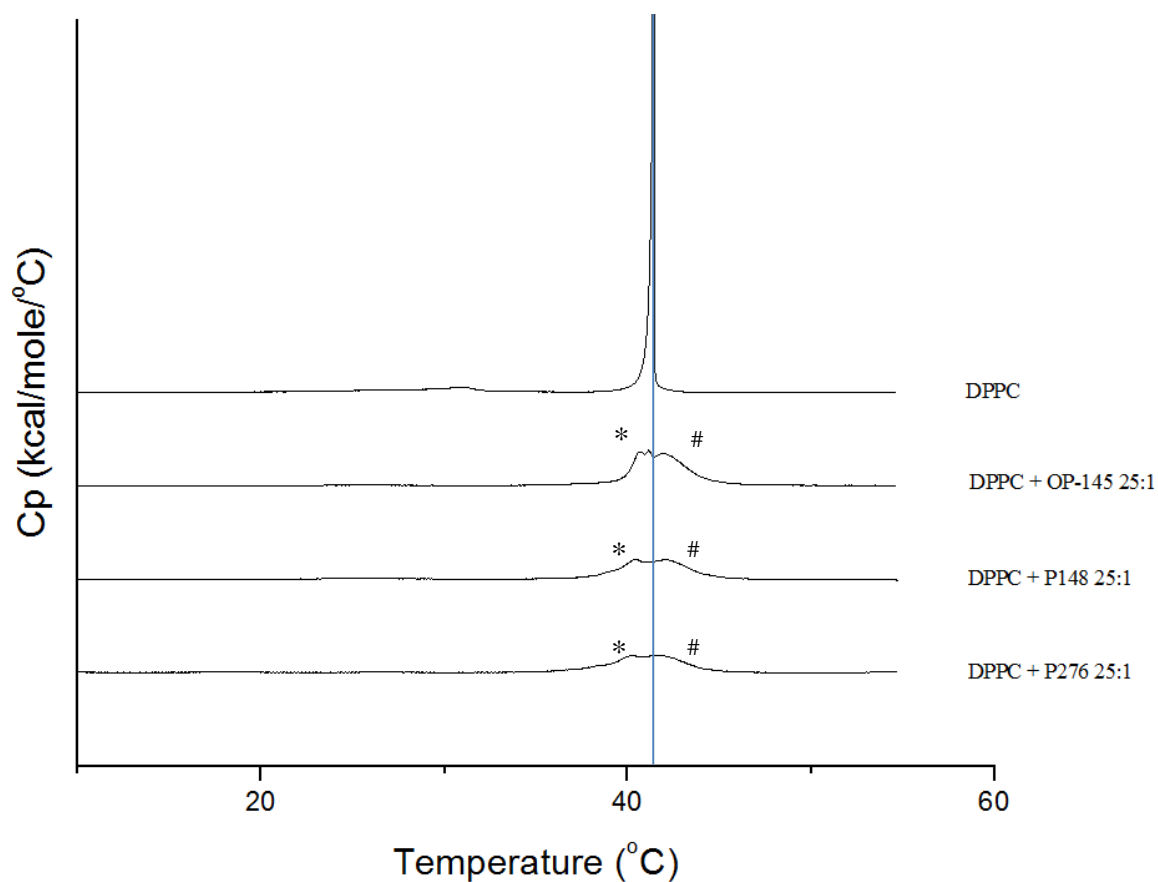
Figure 33. Cooling DSC thermograms of DPPC combined with peptides in molar ratio of 25:1. *peptide rich domain, #peptide poor domain

Table 16. Specific enthalpies and transition temperatures of DPPC vesicles combined with peptides in molar ratio of 25:1 (cooling scans).

		*peptide rich domain			#peptide poor domain	
	Tm (°C)	ΔHm_r (kcal/mol)	$\Delta T1/2$	Tm (°C)	ΔHm_p (kcal/mol)	$\Delta T1/2$
DPPC				41.4	8.1	0.11
OP-145 25:1	40.7	2.1	0.79	41.9	3.7	1.88
P148 25:1	40.4	2.0	1.67	42.1	2.6	2.43
P276 25:1	40.2	1.8	1.70	41.5	2.3	2.47

4.5. VESICLE LEAKAGE ASSAY: IMPACT OF PEPTIDES UPON MEMBRANE PERMEATION

Membrane-disturbing properties of AMPs have been tested on liposomes composed of POPG and POPC with entrapped fluorescent dye ANTS/DPX. The degree of release of fluorescent dye from the vesicles upon incubation with peptides was measured.

Results of leakage assay indicate that all three tested peptides exert a strong activity on POPG membrane (Figure 34). OP-145 may show a bit lower level of activity at lower concentrations, but at 2 μM concentration all peptides have caused a near 100% leakage. The same holds for POPG liposomes with PGN added as there is virtually no difference in comparison to pure POPG (Figure 335). OP-145's activity at lower concentrations seems to have increased a bit, but the significance of this increase is questionable.

As for POPC, OP-145 shows a dramatically lower level of activity with less than 10% leakage caused at the same concentration at which P148 and P276 cause more than 90% leakage (Figure 36). Even at 8 μM OP-145 caused only 40% leakage. With the addition of 25% cholesterol into the membrane, OP-145's activity did not change, while P276 and especially P148 show a slight decrease in their activity, but it was still significantly larger than for OP-145 (Figure 37).
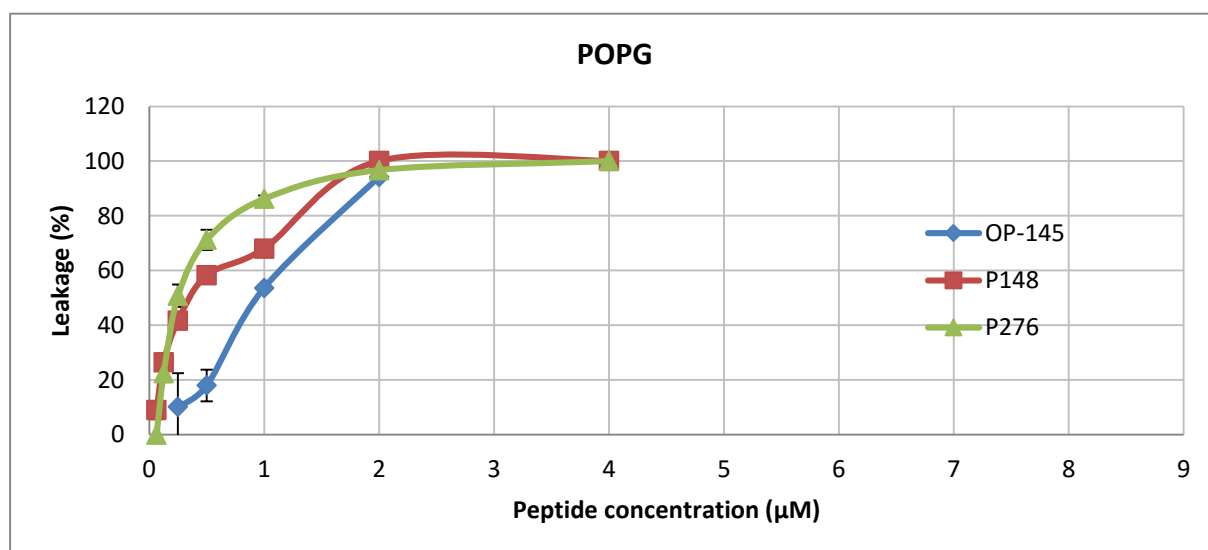

Figure 34. Fluorescent dye leakage from POPG vesicles in interaction with peptides.
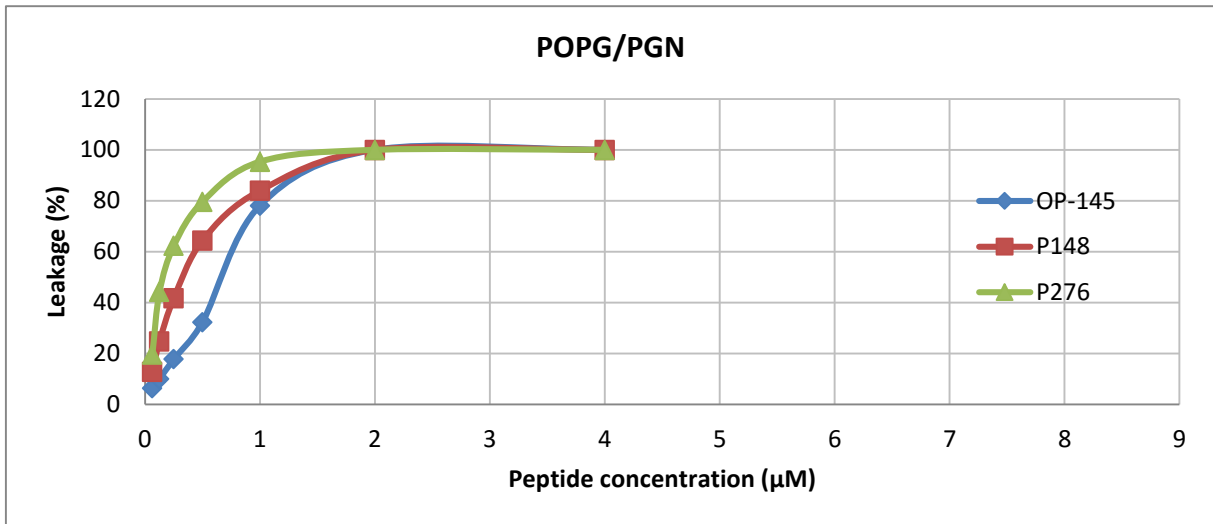
Figure 35. Fluorescent dye leakage from POPG vesicles in presence of PGN in interaction with peptides
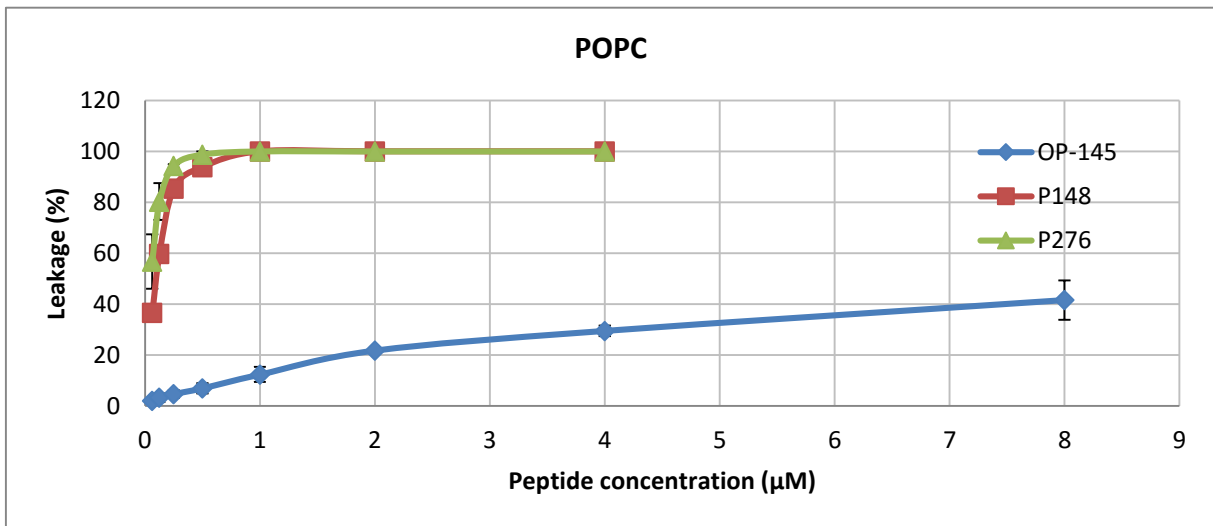
Figure 36. Fluorescent dye leakage from POPC vesicles in interaction with peptides
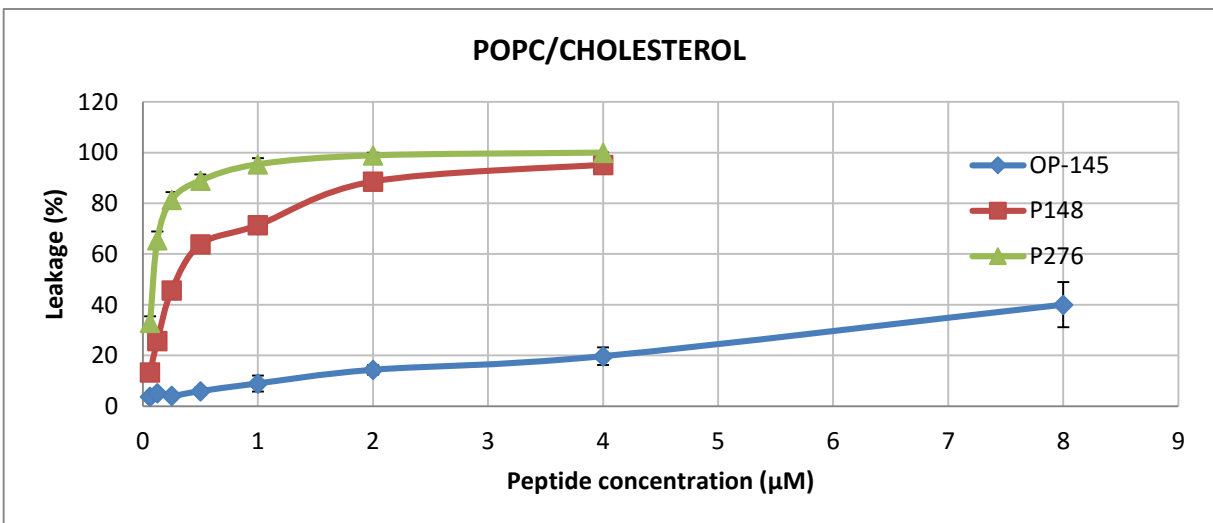
Figure 37. Fluorescent dye leakage from POPC/cholesterol vesicles in interaction with peptides

4.5.1. IMPACT OF SERUM ON MEMBRANE PERMEABILITY ACTION OF AMPs

In order to discern more closely the correlation between AMP's action on model membranes and living cells, leakage assay was also performed in the presence of bovine serum to mimic real organism conditions.

Addition of serum greatly diminishes activity of both tested peptides on POPC membranes (Figure 38), more so of OP-145 than of P148, and the decrease is greater with the increase of serum content. On the other hand, POPG vesicles show complete leakage when serum is added (Figure 39).
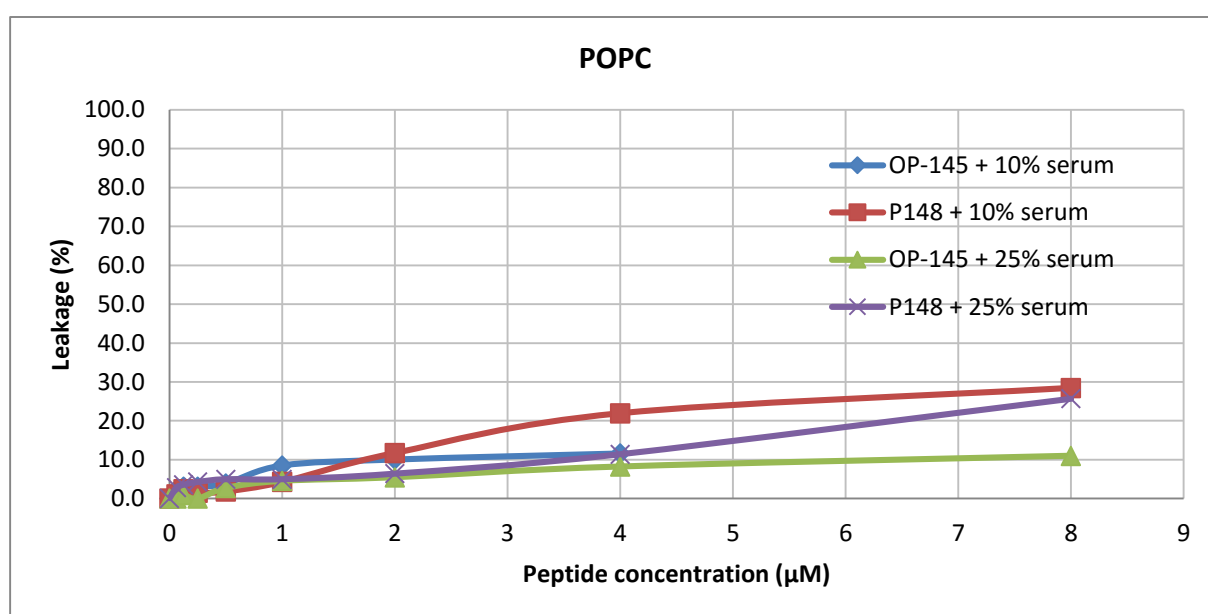
Figure 38. Leakage from POPC vesicles in interaction with peptides in presence of 10% and 25% bovine serum.
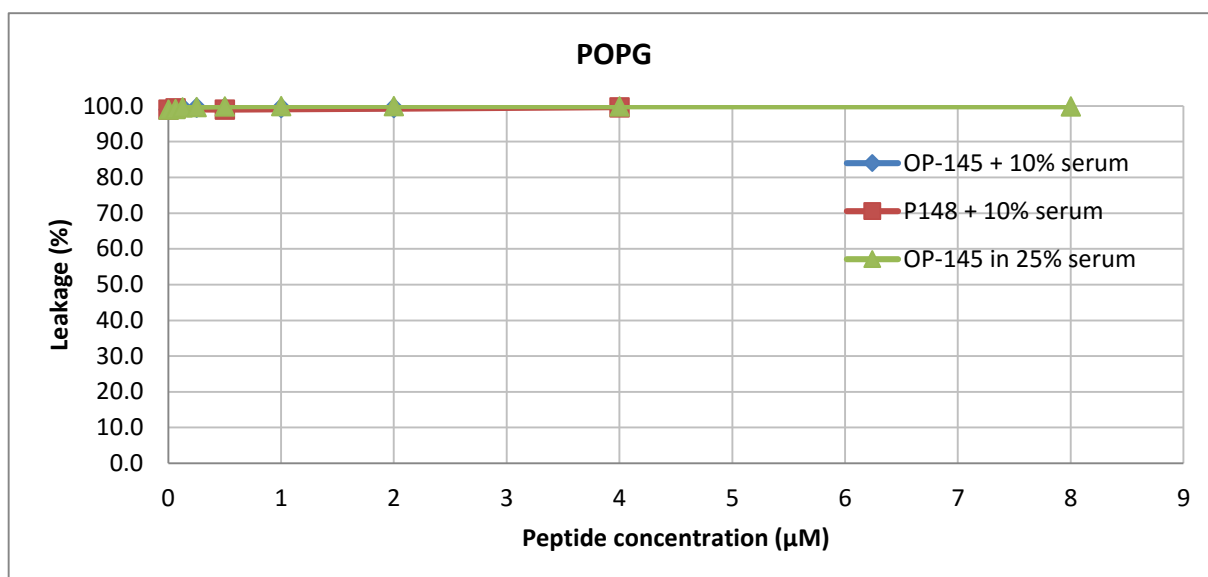
Figure 39. Leakage from POPG vesicles in interaction with peptides in presence of 10% and 25% bovine serum. All values are at 100%.

4.5.2. EFFECT OF BSA ON MEMBRANE PERMEABILITY ACTION OF AMPs

Leakage experiments were performed with bovine serum albumin (BSA) in different concentrations in order to examine the effect of BSA on membrane permeability of AMPs.

Dependence of POPG vesicles leakage on concentration of BSA is nearly linear. Complete leakage is achieved around 5 μM BSA. Contrary to POPG, POPC vesicles show negligible leakage when exposed to pure BSA. Results are shown on Figure 40. Linear fit was calculated using the least squares method. R-squared values are given for reference.
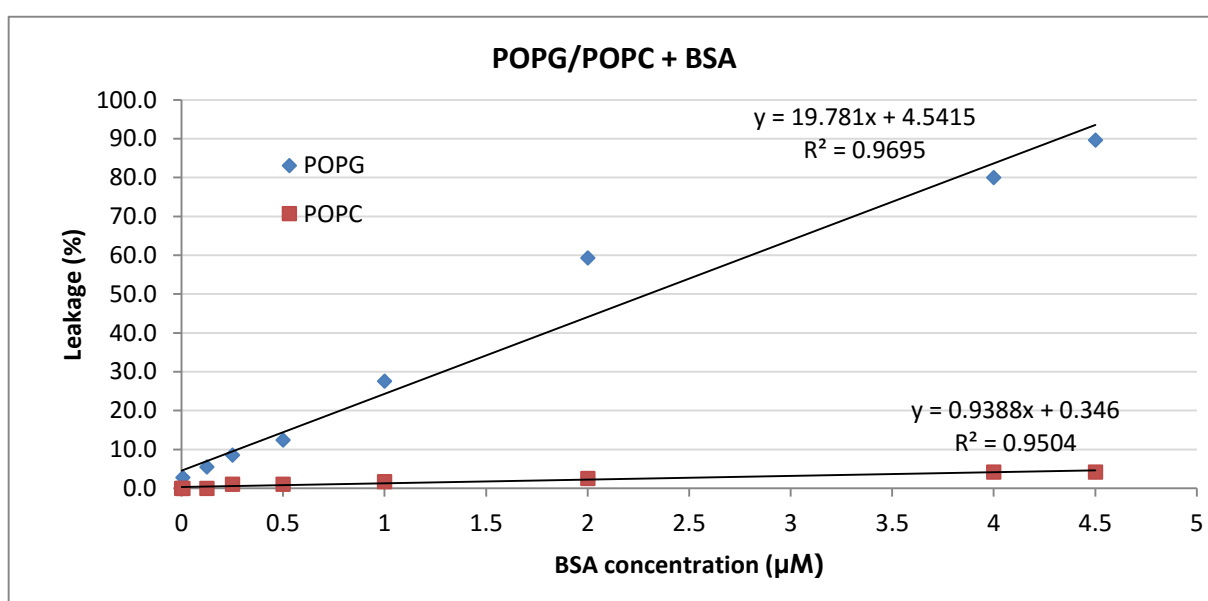
Figure 40. POPG and POPC vesicles leakage in interaction with BSA

4.6. PEPTIDE-LIPID AFFINITY ASSAY: AMPs' DISCRIMINATION BETWEEN MEMBRANES

In order to determine peptides' relative affinity towards PG and PC, an experiment was performed that would show which lipid species is preferred for the peptide to act upon in the presence of both vesicle types.

This experiment showed that OP-145 induces stronger leakage from POPG vesicles even in the presence of POPC. If both species are present in equal concentrations, one labelled and the other not, OP-145 would preferably target POPG (Figure 41). In contrast to this, P148 and P276 show no such selectivity as all leakages from all combinations of liposomes are similar (Figures 42 and 43). It is noteworthy that the total concentration of lipids in mixed POPG/POPC experiments is 100 µM, while in single liposome species experiment it is 50 µM. Therefore, peptide concentrations and molar ratios need to be taken into account when interpreting this data.
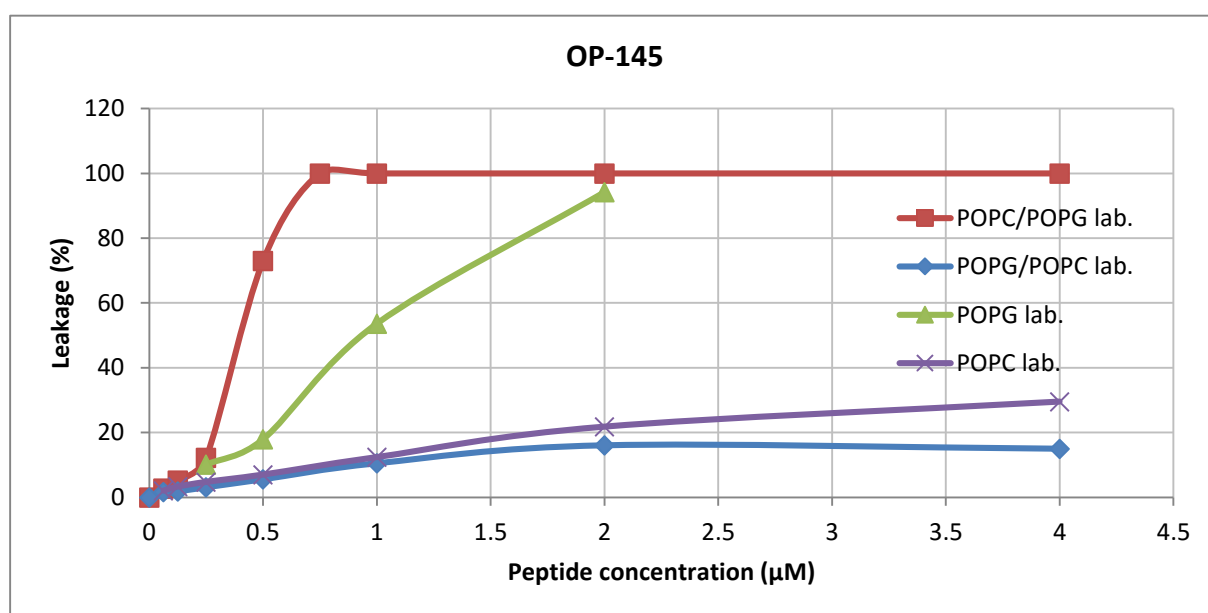
Figure 41. OP-145's affinity towards POPG and POPC vesicles and their combinations
(lab.=fluorescent dye-containing vesicles)

Figure 42. P148's affinity towards POPG and POPC vesicles and their combinations
(lab.=fluorescent dye-containing vesicles)

Figure 43. P276's affinity towards POPG and POPC vesicles and their combinations
(lab.=fluorescent dye-containing vesicles)

5. DISCUSSION

Computer model predictions about secondary structure of OP-145 seem to correspond with what was determined by CD measurements. When dissolved in buffer, OP-145 seems to take its lowest energy conformation (Maupetit, 2009) and does not change it over time. In interaction with SDS micelles and POPG vesicles, 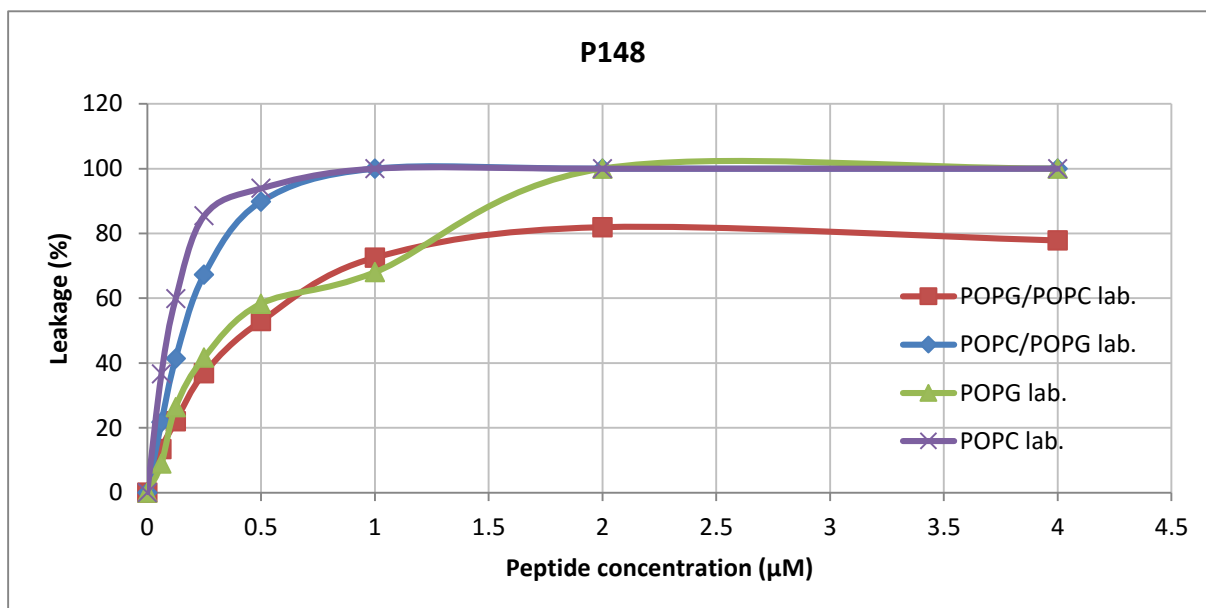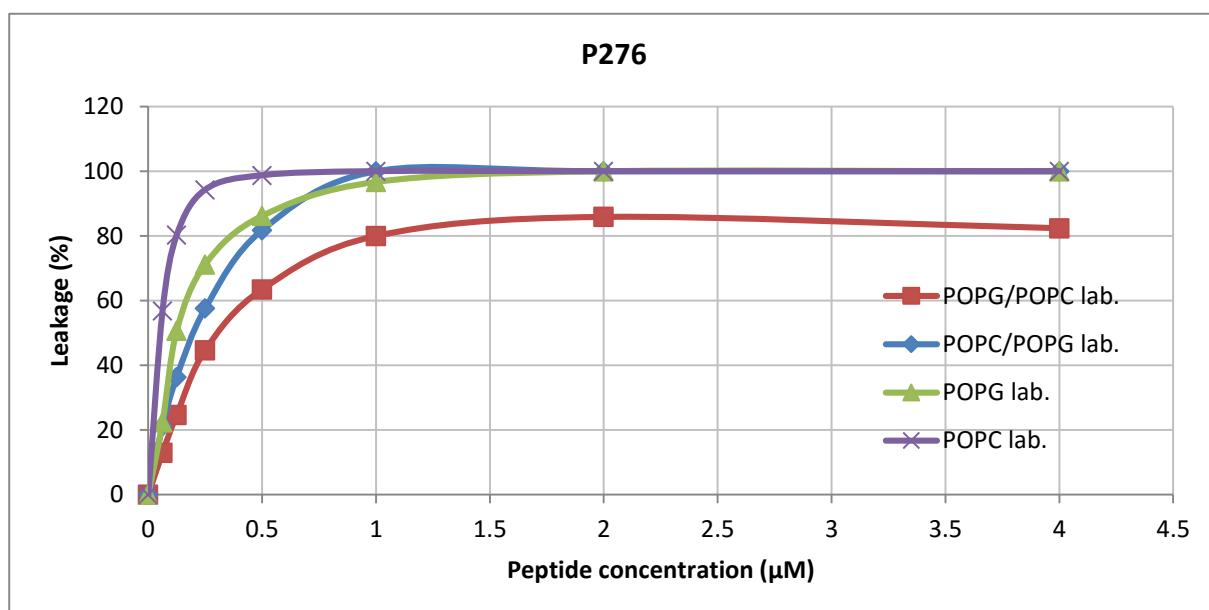which are both prokaryotic model membranes, OP-145 changes its secondary structure: with an increase both in time and in concentration, it becomes less alpha helical, which may be due to the action exerted upon the membrane. Data from size measurements seems to support this premise as POPG vesicles size had increased with an increase both in time and in OP-145 concentration, which might suggest liposome fusion or aggregation under the action of peptides. It could, therefore, be proposed that OP-145 starts its activity upon membranes as an alpha helical peptide and thereafter changes its secondary structure as the membrane degrades and/or fuses to form larger liposomes.

However, previously published data indicates that OP-145 does not take an alpha helical secondary structure in buffer and only does so upon contact with membranes, be it PG or PC, and that it stays alpha helical independent of concentration or the passage of time. Moreover, it indicates that the secondary structure does not influence OP-145's selectivity towards PG and PC membranes (Malanovic et al., 2015). It also indicates that OP-145 induces a quasi-interdigitated state of PG membranes by a planar adherence to the surface with its hydrophobic region, orienting in the interfacial region in a way to shield the acyl chains of the lipid from the aqueous layer (Malanovic et al., 2015; Smith and Dea, 2013). This in turn thins the membrane making it more prone to ruptures. The discrepancy between the results obtained in this study and previously published data could be due to several factors such as peptide oligomerisation during synthesis.

DSC thermograms support the claim that OP-145 and PG (in this case, DPPG) interact as there was a clear shift of the DPPG main transition temperature towards lower value, indicating membrane destabilisation. Moreover, data from leakage assay indicates that OP-145 is active against prokaryotic model membranes as it induces vesicle leakage, as opposed to the eukaryotic model membrane which does not leak as much in the presence of peptide. At 1 µM concentration OP-145 had caused roughly 50% of POPG vesicle leakage, which can be put in correlation with the IC_{50} value for the killing of *S. aureus*, which was 1.6 µM in a 1 h

timeframe (Malanovic et al., 2015). Additionally, it has been shown that the addition of PGN to POPG does not affect the activity of OP-145 towards the membrane, which is confirmed by previous research (Malanovic et al., 2015).

In eukaryotic model membranes, neither OP-145 secondary structure nor vesicle size seems to be affected, suggesting that OP-145 does not interact with DPC and DPPC. However, DSC thermograms disprove this as there is a clear shift in phase transition temperatures and a separation of peaks into the peptide-enriched and peptide-poor domain, as well as a small peak of peptide-free DPPC vesicles at smaller peptide concentrations. This, in turn, has been described by previous research which concluded that the cooperative nature of the underlying transition of the peptide-enriched DPPC domain and its low enthalpy indicated the presence of small disk-like lipid-peptide aggregates or micelles, suggesting that OP-145 exhibits a detergent-like effect on DPPC liposomes (Malanovic et al., 2015). Addition of cholesterol into liposome bilayer does not seem to have an effect on leakage. On the other hand, a considerably lower level of leakage form POPC membranes was observed as compared to POPG, additionally backed up by affinity assays which show that in the presence of both PC and PG vesicles, the level of leakage from PG vesicles is comparable to that of PG vesicles alone, and leakage from PC vesicles is smaller with PG present than from PC vesicles alone. However, leakage from POPC vesicles is still present, indicating possible mammalian cytotoxic activity, which has been shown to exist, albeit in concentrations significantly larger than the ones that exhibit antimicrobial activity, having an $IC_{50} \geq 102.4$ µM for human erythrocytes and ≥ 32 µM for dermal fibroblasts in the presence of 50% plasma (Malanovic et al., 2015).

On top of these results, the presence of bovine serum has shown to reduce the leakage from POPC vesicles, indicating that OP-145 goes into interaction with the serum, possibly binding to serum proteins. Additionally, it has been noticed that the addition of serum alone induces a 100% leakage of POPG vesicles, suggesting that some serum component or components can cause complete disintegration of POPG vesicles. It has been additionally confirmed by conducting an experiment with BSA showing that increasing BSA concentrations nearly linearly increase the degree of leakage from POPG vesicles, with roughly 5 µM BSA causing almost 100% leakage. Given that BSA concentration in bovine serum is around 35 g/l (Matei et al., 2010), with molar mass of 66430 g/mol (Hirayama et al., 1990), which gives a molar concentration of 527 µM, even a 10% serum solution would still contain more than 10 times

the concentration of BSA needed to cause complete leakage, which indicates that it is a viable hypothesis that BSA can cause POPG disintegration.

As opposed to OP-145, which has been researched previously, P148 and P276 have only been tested for antimicrobial activity and there is no previously published data on their biophysical properties. They are, therefore, compared to their parental peptide OP-145. Although P148 and P276 only differ in one amino acid, they do differ in their properties. It has been shown before that a point mutation in a short-chain AMP can cause radically different properties (Malanovic et al., 2014).

P148 and P276 have net charges of +11 and +10, respectively, at pH=7.0, as compared to OP-145 which has a net charge of +6. They are also designed in a way to have improved amphipathic character. Based on these properties alone it can be predicted that both P148 and P276 adhere to PG vesicles stronger than OP-145, given PG's negative charge. This could in turn mean stronger initial interactions with membrane phospholipids. In addition, their higher hydrophobicity can induce higher level of partitioning into the hydrophobic bilayer. Taking the hydrophobicity into account, their improved amphipathic character could cause a stronger action against PC membranes, as there would be no electrostatic repulsions between the positive peptide and zwitterionic PC and the hydrophobic part of the peptide could more easily penetrate into the bilayer, causing disaggregation of multilamellar organization of PC membranes.

The secondary structures predicted by computer models do not correspond to the ones determined by CD. Hence we may assume that alpha helical secondary structure is not the lowest energy conformation for these two peptides when they are dissolved in PBS, nor that it is necessary for the peptide to take an alpha helical conformation to exert action upon the membranes. P148, however, adopts rather alpha helical structure in SDS, which diminishes in time and with the increase of peptide concentration relative to lipid. In DPC the secondary structure seems to be rather stable and to larger extent alpha helical, but in PG and PC vesicles alpha helicity seems to diminish. P276 seems to have a larger proportion of alpha helix in its structure when interacting with SDS, DPC, and PG, but not with PC vesicles. There is no change in PC vesicle size present, with only slight changes in PG vesicles size. As for the DSC, P276 shows stronger main transition temperature shift of POPG vesicles than P148, comparable to that of OP-145, suggesting membrane destabilisation. Both peptides

seem to cause a complete disappearance of the pretransition in POPG at a lipid:peptide ratio of 50:1 and smaller (meaning larger peptide concentrations), which might indicate stabilisation of the untilted gel phase. As for the interaction with POPC, phase separation is again present as was the case with OP-145. However, transition enthalpies are significantly lower than those exhibited with OP-145, again stronger with P276, suggesting almost total liposome disaggregation.

Considering the leakage assay, it can be deduced that neither P148 nor P276 discriminate between PG and PC membranes, suggesting a larger degree of mammalian cell lysis, which is confirmed by haemolytic activity tests (see Table 2, section 1.2). However, in the presence of serum, P148 activity on PC vesicles drops significantly to around 20% leakage at 4 μM concentration with 10% serum and 10% leakage at the same concentration with 25% serum. It can be speculated that with 50% serum it would drop considerably, as was the case with haemolytic activity test where MMNHC was 12.8 μM. This suggests that, although in PBS P148 exerts a strong negative activity on mammalian cells, it could discriminate between bacterial and mammalian cells in physiological conditions with good activity against bacteria and minimum harm to the organism. Data for PG vesicles was unavailable due to the previously described lysis in the presence of serum. Adding PGN to PG vesicles has no effect on leakage induced by these two peptides, as it had no influence on the activity of OP-145, suggesting that bacterial cell wall (especially that of Gram-positive bacteria) would not impede the peptides' action. It can be speculated that the addition of cholesterol into PC membrane reduces P148's affinity towards the membrane slightly, although, as in the case with OP-145, the statistical significance is unclear. If this is the case, it would additionally provide support to the claim that P148 has lower affinity towards mammalian cells.

All data combined indicates that P148 and P276 exhibit action against both bacterial and mammalian model membranes in buffer. However, with the addition of serum, P148's selectivity towards prokaryotic membrane largely increases. It could be speculated that a similar change in activity would have been detected with P276 if analysed. When compared to OP-145, both peptides show stronger action against both bacterial and mammalian model membranes, but in the presence of serum, that difference largely disappears. P276 comparatively shows biophysical properties more similar to those of OP-145 than P148 and, as determined from antibacterial assays, is more potent against Gram-positive bacteria than P148 in the presence of plasma.

6. CONCLUSION

Prokaryotic and eukaryotic model membranes were subjected to a series of analyses under the influence of antimicrobial peptides OP-145, P148 and P276, concurrently assessing the properties of these peptides. They have shown to influence the membranes in such a way that causes increased tendency towards destabilisation and disruption. They have shown to possess antimicrobial as well as haemolytic activity, both on model membranes and, as previously established, on living cells, P148 and P276 more than OP-145; haemolytic and mammalian model membrane activity being largely diminished with the addition of blood serum. P148 and especially P276 have shown stronger interaction with membrane phospholipids than OP-145. P276 has shown to have a more alpha helical structure than P148, although both lesser than OP-145.

On the basis of the data obtained in biophysical experiments on model membranes performed for this thesis, as well as previously published data, in accordance with this thesis' objectives, it can be concluded that P148 and especially P276 have better biophysical properties than OP-145 in terms of antimicrobial activity. However, further research is needed to fully understand their properties, safety, efficacy and their potential use as antimicrobial agents.

7. REFERENCES

Arouri A, Dathe M, Blume A. The helical propensity of KLA amphipathic peptides enhances their binding to gel-state lipid membranes. *Biophys Chem*, 2013, 180-181, 10-21.

Atkins P, de Paula J. Atkins' Physical Chemistry, 8th ed. New York, W. H. Freeman and Company, 2006, pp. 46, 490, 675-679, 849-850.

Bartlett GR. Colorimetric assay methods for free and phosphorylated glyceric acids. *J Biol Chem*, 1959, 234, 469-471.

Batoni G, Maisetta G, Esin S. Antimicrobial peptides and their interaction with biofilms of medically relevant bacteria. *Biochim Biophys Acta*, 2016, 1858(5), 1044-1060.

Antimicrobial peptides, Biofilms. http://www.bali-consortium.eu, accessed 25 September 2016.

Bucki R, Namiot DB, Namiot Z, Savage PB, Janmey PA. Salivary mucins inhibit antibacterial activity of the cathelicidin-derived LL-37 peptide but not the cationic steroid CSA-13. *J Antimicrob Chemother*, 2008, 62(2), 329-335.

Antibiotic resistance threats in the United States, 2013, http://www.cdc.gov, accessed 4 November 2015.

Compton L, Johnson WJ. Analysis of protein circular dichroism spectra for secondary structure using a simple matrix multiplication. *Anal Biochem,* 1986, 155(1), 155-167.

de Breij A, Riool M, Kwakman PH, de Boer L, Cordfunke RA, Drijfhout JW, Cohen O, Emanuel N, Zaat SA, Nibbering PH, Moriarty TF. Prevention of Staphylococcus aureus biomaterial-associated infections using a polymer-lipid coating containing the antimicrobial peptide OP-145. *J Control Release*, 2016, 222, 1-8.

Dürr U, Sudheendra U, Ramamoorthy A. LL-37, the only human member of the cathelicidin family of antimicrobial peptides. *Biochim Biophys Acta*, 2006, 1758(9), 1408-1425.

Ellens H, Bentz J, Szoka F. H+- and Ca2+-induced fusion and destabilization of liposomes. *Biochemistry*, 1985, 24(13), 3099-3106.

Haisma EM, de Breij A, Chan H, van Dissel JT, Drijfhout JW, Hiemstra PS, El Ghalbzouri A, Nibbering PH. LL-37-derived peptides eradicate multidrug-resistant Staphylococcus aureus from thermally wounded human skin equivalents. *Antimicrob Agents Chemother*, 2014, 58(8), 4411-4419.

Hancock R, Sahl H. Antimicrobial and host defense peptides as new anti-infective therapeutic strategies. *Nat Biotechnol*, 2006, 24, 1551-1557.

Hirayama K, Akashi S, Furuya M, Fukuhara K. Rapid confirmation and revision of the primary structure of bovine serum albumin by ESIMS and Frit-FAB LC/MS. *Biochem Biophys Res Commun*, 1990, 173(2), 639-646.

Koller D, Lohner K. The role of spontaneous lipid curvature in the interaction of interfacially active peptides with membranes. *Biochim Biophys Acta*, 2014, 1838(9), 2250-2259.

Lohner K. New strategies for novel antibiotics: peptides targeting bacterial cell membranes. *Gen Physiol Biophys,* 2009, 28(2), 105-116.

Lohner K, Prenner E. Differential scanning calorimetry and X-ray diffraction studies of the specificity of the interaction of antimicrobial peptides with membrane-mimetic systems. *Biochim Biophys Acta*, 1999, 1462(1-2), 141-156.

Lohner K, Sevcsik E, Pabst G. Liposome-Based Biomembrane Mimetic Systems: Implications for Lipid-Peptide Interactions. In: Advances in Planar Lipid Bilayers and Liposomes, Volume 6. Leitmannova Liu A, Tien H, editors, Academic Press, 2008, pp. 103-137.

Malanovic N, Drijfhout JW, Kriechbaum M, Schmuck M, de Breij A, Nibbering PH, Lohner K. Point mutation in the hydrophobic region drives selectivity and activity of OP-145, a derivative of human cathelicidin LL-37. *Biophys J*, 2014, 106(2), 442a.

Malanovic N, Leber R, Schmuck M, Kriechbaum M, Cordfunke RA, Drijfhout JW, de Breij A, Nibbering PH, Kolb D, Lohner K. Phospholipid-driven differences determine the action of

the synthetic antimicrobial peptide OP-145 on Gram-positive bacterial and mammalian membrane model systems. *Biochim Biophys Acta*, 2015, 1848(10 Pt A), 2437-2447.

Malanovic N, Lohner K. Gram-positive bacterial cell envelopes: The impact on the activity of antimicrobial peptides. *Biochim Biophys Acta*, 2016, 1858(5), 936-946.

Dynamic Light Scattering (DLS), 2016, http://www.malvern.com, accessed 25 September 2016.

Manzo G, Carboni M, Rinaldi AC, Casu M, Scorciapino MA. Characterization of sodium dodecylsulphate and dodecylphosphocholine mixed micelles through NMR and dynamic light scattering. *Magn Reson Chem*, 2013, 51(3), 176-183.

Matei ST, Groza I, Andrei S, Bogdan L, Ciupe S, Petrean A. Serum metabolic parameters in healthy and subclinical mastitis cows. *Bulletin of University of Agricultural Sciences and Veterinary Medicine Cluj-Napoca. Veterinary Medicine*, 2010, 67(1).

Maupetit J, Derreumaux P, Tuffery P. PEP-FOLD: an online resource for de novo peptide structure prediction. *Nucleic Acids Res*, 2009, 37, W498-503.

Nell MJ, Tjabringa GS, Wafelman AR, Verrijk R, Hiemstra PS, Drijfhout JW, Grote JJ. Development of novel LL-37 derived antimicrobial peptides with LPS and LTA neutralizing and antimicrobial activities for therapeutic application. *Peptides*, 2006, 27(4), 649-660.

Néron B, Ménager H, Maufrais C, Joly N, Maupetit J, Letort S, Carrere S, Tuffery P, Letondal C. Mobyle: a new full web bioinformatics framework. *Bioinformatics*, 2009, 25(22), 3005-3011.

Nibbering PH, de Breij A, Cordfunke RA, Zaat SAJ, Drijfhout JW. 2015. EU Patent WO/2015/088344.

Peek FAW, Nell MJ, Brand R, Jansen-Werkhoven TM, van Hoogdalem EJ, Frijns JHM. Double-blind placebo-controlled study of the novel peptide drug P60.4Ac in chronic middle ear infection. 49th Intersci Conf Antimicrob Agents Chemother, San Francisco, 2009.

CD Units & Conversions, 2015, http://www.photophysics.com, accessed 25 September 2016.

Reddy K, Yedery R, Aranha C. Antimicrobial peptides: premises and promises. *Int J Antimicrob Agents*, 2004, 24(6), 536-547.

Riedl S, Leber R, Rinner B, Schaider H, Lohner K, Zweytick D. Human lactoferricin derived di-peptides deploying loop structures induce apoptosis specifically in cancer cells through targeting membranous phosphatidylserine. *Biochim Biophys Acta*, 2015, 1848(11 Pt A), 2918-2931.

Shen Y, Maupetit J, Derreumaux P, Tufféry P. Improved PEP-FOLD Approach for Peptide and Miniprotein Structure Prediction. *J Chem Theory Comput*, 2014, 10(10), 4745-4758.

Smith EA, Dea PK. Differential Scanning Calorimetry Studies of Phospholipid Membranes: The Interdigitated Gel Phase. In: Applications of Calorimetry in a Wide Context - Differential Scanning Calorimetry, Isothermal Titration Calorimetry and Microcalorimetry. Elkordy AA, editor, Rijeka, InTech, 2013, pp. 407-444.

Sørensen O, Arnljots K, Cowland JB, Bainton DF, Borregaard N. The human antibacterial cathelicidin, hCAP-18, is synthesized in myelocytes and metamyelocytes and localized to specific granules in neutrophils. *Blood*, 1997, 90(7), 2796-2803.

Stano P, Bufali S, Domazou A, Luisi P. Effect of tryptophan oligopeptides on the size distribution of POPC liposomes: a dynamic light scattering and turbidimetric study. *J Liposome Res*, 2005, 15(1-2), 29-47.

Vert M, Doi Y, Hellwich KH, Hess M, Hodge P, Kubisa P, Rinuado M, Schue F. Terminology for biorelated polymers and applications (IUPAC Recommendations 2012). *Pure Appl Chem*, 2012, 84(2), 377-410.

Watson DG. Pharmaceutical Analysis. A Textbook for Pharmacy Students and Pharmaceutical Chemists, 1st ed. Edinburgh, Hartcourt Publishers Limited, 1999, pp. 133-139.

Whitmore L, Wallace B. DICHROWEB: an online server for protein secondary structure analyses from circular dichroism spectroscopic data. *Nucleic Acids Research*, 2004, 32, 668-673.

At UN, global leaders commit to act on antimicrobial resistance, 2016, http://www.who.int, accessed 25 September 2016.

WHO. Global action plan on antimicrobial resistance, 2015, http://www.who.int, accessed 25 September 2016.

World Bank. Drug-Resistant Infections: A Threat to Our Economic Future (Discussion Draft), 2016, http://www.worldbank.org, accessed 25 September 2016.

Zanetti M, Gennaro R, Romeo D. Cathelicidins: a novel protein family with a common proregion and a variable C-terminal antimicrobial domain. *FEBS Lett*, 1995, 374(1), 1-5.

Zasloff M. Antimicrobial peptides of multicellular organisms. *Nature*, 2002, 415, 389-395.

Zweytick D, Deutsch G, Andrä J, Blondelle SE, Vollmer E, Jerala R, Lohner K. Studies on lactoferricin-derived Escherichia coli membrane-active peptides reveal differences in the mechanism of N-acylated versus nonacylated peptides. *J Biol Chem*, 2011, 286(24), 21266-21276.

8. SUMMARY

Antimicrobial peptides (AMPs) are a novel class of therapeutics with activity against pathogens. Of special interest are AMPs that act against bacteria. Such peptides mostly act by disrupting bacterial cytoplasmic membrane. Therefore, membrane composition as well as peptide properties are both important in determining a peptide's level of activity. Such peptides may show other properties such as immunomodulation and antibiofilm activity, but can also have disadvantages such as toxicity towards mammalian cells. Therefore, new peptides with better and enhanced properties are being developed as new potential therapeutics. In Biofilm Alliance, an international consortium, such new peptides are being developed and modelled after OP-145, an AMP derived from LL-37, which is a naturally occurring cathelicidin-derived antimicrobial peptide found in humans. Among these new peptides are P148 and P276, whose properties have been studied in this thesis. The goal was to compare their properties to those of OP-145.

To gain insight into their mode of action, OP-145, P148 and P276 were subjected to a series of test which included *in silico* modelling and investigation of their interactions with prokaryotic and eukaryotic model membranes by terms of thermoanalytical measurements using DSC, measurements of size of model membrane vesicles in interaction with peptides using DLS, determination of peptides' secondary structure both alone and in interaction with membranes using CD and quantitative research of the peptides' ability to disrupt these membranes in the form of leakage assays using fluorometry. Data gained from these experiments was then compared to previously known properties of these peptides.

It was determined that OP-145 has a more alpha helical secondary structure than P148 and P276, but it was concluded that the secondary structure is not necessarily a factor of their action. The results stipulated that P148 and P276 exerted stronger action on both model membranes than OP-145, as was shown in calorimetric measurements and vesicle leakage assays. It was also shown that P148 and P276 have stronger activity than OP-145 against both bacterial and mammalian model membranes in the presence of blood serum. Previously known data suggests that P148 and P276 are more active against bacteria in the presence of blood serum than OP-145, with toxicity towards mammalian cells within acceptable limits. It was concluded that P148 and especially P276 have better biophysical properties than OP-145 in terms of antimicrobial activity, but that further research is needed in order to better understand their properties and possible therapeutic use.

9. SAŽETAK

9.1. UVOD

S porastom antimikrobne rezistencije u svijetu pojavljuje se potreba za novim antimikrobnim tvarima, posebice novim antibioticima. Jedan od pristupa je i istraživanje antimikrobnih peptida (AMP). Ti peptidi su često dio obrambenog sustava različitih organizama, a ti prirodni spojevi se mogu koristiti kao modeli za razvoj novih, sintetskih antimikrobnih peptida s poboljšanim svojstvima kao što su imunomodulacijsko djelovanje ili djelovanje protiv biofilma. Biofilm Alliance (BALI) je međunarodni istraživački konzorcij koji razvija nove antimikrobne peptide koristeći OP-145 kao model. OP-145 je AMP razvijen iz LL-37, humanog antimikrobnog peptida prisutnog u raznim tkivima, koji nastaje iz hCAP-18 iz porodice katelicidina. Među tim peptidima razvijenima unutar projekta BALI su i P148 i P276 čija svojstva su istraživana u ovome radu.

U literaturi je opisano da je glavni mehanizam djelovanja antimikrobnih peptida interakcija sa staničnom membranom bakterija pri čemu dolazi do njezine destabilizacije i dezintegracije ili do formiranja pora, što oboje dovodi do curenja staničnog sadržaja i smrti bakterijske stanice. Stoga je važno shvatiti na koji način takvi peptidi ulaze u te interakcije. Budući da su prave biološke membrane kompleksan skup različitih lipida, proteina i polisaharida, postoji potreba za njihovim pojednostavljenjem kako bi se lakše istražile interakcije između AMP i membrana. Često se kao model za bakterijske membrane koriste liposomi ili vezikule sastavljene od fosfatidilglicerolnih lipida (PG), dok se kao modeli za eukariotske membrane koriste fosfatidilkolinski lipidi, aproksimirajući time ugrubo sastav pravih bioloških membrana.

9.2. OBRAZLOŽENJE TEME

Cilj ovoga rada bio je otkriti biofizikalna svojstva antimikrobnih peptida P148 i P276 i usporediti ih sa svojstvima peptida na temelju kojega su razvijeni, OP-145. Pritom su istraživane njihove interakcije s modelima bioloških membrana. Svrha rada je bila doprinijeti spoznaji o antimikrobnim peptidima i općenito razvoju novih antimikrobnih tvari, boreći se time protiv rastućeg problema antimikrobne rezistencije.

9.3. MATERIJALI I METODE

U eksperimentima koji su provedeni za izradu ovog diplomskog rada korištene su sljedeće metode: diferencijalna pretražna kalorimetrija (DSC) za otkrivanje termodinamičkih promjena u lipidima pri kontaktu s antimikrobnim peptidima; cirkularni dikroizam (CD) za ispitivanje sekundarne strukture peptida u interakciji s lipidima i samih peptida; dinamičko raspršenje svjetlosti (DLS) za mjerenje veličine liposoma kao funkcije vremena u kontaktu s peptidima i fluorometrija za mjerenje curenja fluorescentnog sadržaja iz liposoma zbog degradacije membrane pod utjecajem peptida. Liposomi za DSC su pripravljeni od DPPG-a (dipalmitoilfosfatidilglicerol) i DPPC-a (dipalmitoilfosfatidilkolin), dok su liposomi za CD, DLS i fluorometriju pripravljeni od POPG-a i POPC-a (palmitoil-oleil-fosfatidilglicerol/kolin). Potonji su ekstrudirani kroz membranske filtere da bi se dobile unilamelarne vezikule (jedan lipidni dvosloj) te radi homogenosti veličina. Zatim su podvrgnuti ispitivanju navedenim tehnikama uz dodatak peptida u različitim koncentracijama te su promatrana njihova svojstva i svojstva peptida ovisno o koncentraciji peptida i vremenu. Također su provedena računalna modeliranja za procjenu sekundarne strukture peptida.

9.4. REZULTATI, RASPRAVA I ZAKLJUČAK

Dobiveni rezultati pokazali su kako OP-145 posjeduje sekundarnu strukturu alfa heliksa, dok P148 i P276 nisu pokazali takva svojstva, što je bilo u suprotnosti s računalnim modelima koji su pokazali veliki udio alfa heliksa u sva tri peptida. U interakciji s membranama, peptidi su se različito ponašali: od promjene udjela alfa heliksa u ovisnosti o koncentraciji peptida i vremenu do potpunog izostanka alfa heliksa u sek. strukturi. Zaključeno je, a i sugerirano u prijašnjim istraživanjima, da alfa heliks nije nužan uvjet za antimikrobnu aktivnost. Mjerenje veličine liposoma je pokazalo da veličina POPG vezikula raste s porastom koncentracije OP-145 i protekom vremena; predloženo je da je moglo doći do fuzije ili agregacije liposoma. Međutim, u dosadašnjim istraživanjima OP-145 nije pokazao takvo djelovanje na vezikule. Nije došlo do promjene veličine liposoma u ostalim slučajevima. DSC je pokazao značajne pomake u temperaturama faznih pomaka lipida u kontaktu s peptidima, to veće pomake što je veća koncentracija peptida, kao i razdvajanje signala u više pikova, što sugerira da su interakcije dosta snažne. Test curenja je pokazao da P148 i P276 uzrokuju jače curenje, odnosno dezintegraciju membrane POPG i pogotovo POPC vezikula od OP-145, što bi značilo podjednaku aktivnost na bakterijskim modelnim membranama kao i OP-145, ali i

mnogo jaču aktivnost na eukariotskim membranama, što ukazuje na moguću toksičnost. Također je ukazao da, kad se pokus izvodi u puferu, P148 i P276 ne pokazuju razliku u djelovanju prema PG i PC membranama, dok OP-145 puno jače djeluje na PG od PC. Međutim, dodatkom krvnog seruma smanjuje se djelovanje na obje vrste membrana, a pritom u literaturi nalazimo podatke o antibakterijskoj aktivnosti i hemolitičkoj aktivnosti P148 i P276 koji ukazuju na činjenicu da je koncentracija peptida koja ubija bakterije ispod hemolitičke koncentracije, što sugerira potencijal za veću sigurnost upotrebe P148 i P276 od OP-145 kojemu u prisutnosti krvnog seruma uvelike opada antibakterijska aktivnost.

Na kraju je zaključeno da P148 i pogotovo P276 pokazuju bolja biofizikalna svojstva od OP-145 u kontekstu antimikrobne aktivnosti, ali da su isto tako potrebna daljnja istraživanja da bi se točno ustanovilo koliki je njihov potencijal za daljnju primjenu.

10. APPENDIX - LIST OF ABBREVIATIONS

AMP(s) – antimicrobial peptide(s)

AMR – antimicrobial resistance

ANTS – 8-aminonaphthalene-1,3,6-trisulfonic acid, a fluorophore

BALI – Biofilm Alliance (www.bali-consortium.eu)

BSA – bovine serum albumin

CD – circular dichroism

DLS – dynamic light scattering

DPC - dodecylphosphocholine

DPPC – dipalmytoilphosphatidylcholine, lipid in mammalian model membranes

DPPG – dipalmytoilphosphatidylglycerol, lipid in bacterial model membranes

DPX – p-xylene-bis-pyridinium bromide, fluorescence quencher

DSC – differential scanning calorimetry

hCAP-18 – a human cathelicidin which gives LL-37 after cleavage with proteases

HEPES - 4-(2-hydroxyethyl)piperazine-1-ethanesulfonic acid, organic buffering agent

IC50 – inhibitory concentration that inhibits the growth of 50% of bacteria

LC99.9 – lethal concentration of an antimicrobial agent that kills 99.9% of bacteria

LL-37 – an AMP derived from hCAP-18; used as a model for OP-145

LPS – lipopolysaccharide

LTA – lipoteichoic acid

MDR – multiple drug resistance

MMNHC - median maximal non-haemolytic concentration

MRSA – methicillin-resistant *S. aureus*

MV – multilamellar vesicles

OP-145 – an AMP derived from LL-37; used as a model in BALI project for the development
   of new AMPs

OV – oligolamellar vesicles

P148 – an AMP developed from OP-145

P276 – an AMP developed from OP-145

P60.4Ac – old name for OP-145

PBS – phosphate-buffered saline

PC – phosphatidylcholine

PDI – polydispersity index

PE – phosphatidylethanolamine

PG – phosphatidylglycerol

PGN – peptidoglycan

POPC – palmytoil-oleil-phosphatidylcholine, lipid in mammalian model membranes

POPG – palmytoil-oleil-phosphatidylglycerol, lipid in bacterial model membranes

PS – phosphatidylserine

QELS – quasi-elastic light scattering (other name for DLS)

SDS – sodium dodecylsulfate (a.k.a. sodium lauryl sulfate)

SM – sphingomyelin

UV – unilamellar vesicles

WHO – World Health Organisation

BIOPHYSICAL CHARACTERISATION OF LL-37-DERIVED ANTIMICROBIAL PEPTIDES

Drago Ilišinović

SUMMARY

Antimicrobial peptides (AMPs) are a novel class of therapeutics with activity against bacteria. Such peptides mostly act by disrupting bacterial cytoplasmic membrane. Therefore, membrane composition as well as peptide properties are both important in determining a peptide's level of activity. Such peptides may have both positive and negative additional properties. Therefore, new peptides with better and enhanced properties are being developed. One of such peptides is OP-145, derived from LL-37. From OP-145, new AMPs were developed, including P148 and P276, which were researched in this thesis. OP-145, P148 and P276 were subjected to a series of test which included *in silico* modelling and investigation of their interactions with prokaryotic and eukaryotic model membranes by terms of thermoanalytical measurements using DSC, measurements of size of model membrane vesicles in interaction with peptides using DLS, determination of peptides' secondary structure in interaction with membranes using CD and quantitative research of the peptides' ability to disrupt these membranes in the form of leakage assays using fluorometry. Data gained from these experiments was then compared to previously known properties of the peptides. Results have shown a stronger level of activity of P148 and P276 in comparison to OP-145 towards both bacterial and mammalian model membranes. It was concluded that P148 and P276 have better biophysical properties than OP-145 in terms of antimicrobial activity, but that further research is needed in order to better understand their properties and possible therapeutic use.

BIOFIZIKALNA KARAKTERIZACIJA ANTIMIKROBNIH PEPTIDA IZVEDENIH IZ LL-37

Drago Ilišinović

SAŽETAK

Antimikrobni peptidi (AMP) su nova klasa terapeutika s antibakterijskom aktivnošću. Način djelovanja tih peptida je većinom narušavanje integriteta stanične membrane. Stoga su i sastav membrane i svojstva peptida važni za utvrđivanje stupnja aktivnosti peptida. Takvi peptidi mogu imati i dodatna svojstva, pozitivna i negativna. Stoga se razvijaju novi peptidi s poboljšanim svojstvima. Jedan od takvih peptida je i OP-145 koji je razvijen iz LL-37. Iz OP-145 su razvijeni novi antimikrobni peptidi, uključujući P148 i P276 koji su istraživani u ovom radu. OP-145, P148 i P276 su podvrgnuti nizu ispitivanja uključujući *in silico* modeliranje i istraživanje njihovih interakcija s prokariotskim i eukariotskim modelnim membranama koristeći termoanalitičke metode (DSC), mjerenje veličina vezikula modelnih membrana koristeći DLS, određivanje sekundarne strukture peptida u interakciji s modelnim membranama koristeći CD i određivanje stupnja aktivnosti prema membranama mjereći curenje fluorescentnog sadržaja iz vezikula. Dobiveni podaci su uspoređeni s otprije poznatim svojstvima tih peptida. Rezultati su pokazali povećan stupanj aktivnosti P148 i P276 u usporedbi s OP-145 prema prokariotskim i eukariotskim modelnim membranama. Zaključeno je da P148 i P276 imaju bolja biofizikalna svojstva od OP-145 u smislu antimikrobne aktivnosti, ali i da su potrebna daljnja istraživanja tih peptida kako bi se bolje utvrdila njihova svojstva i mogućnost primjene.